Journal of Pharmaceutical Analysis 15 (2025) 101095

Contents lists available at ScienceDirect

Journal of Pharmaceutical Analysis

journal homepage: www.elsevier.com/locate/jpa

Review paper

Urease-powered micro/nanomotors: Current progress and challenges

Wen-Wen Li [a], Zi-Li Yu [a, b, *], Jun Jia [a, b, **]

[a] State Key Laboratory of Oral & Maxillofacial Reconstruction and Regeneration, Key Laboratory of Oral Biomedicine Ministry of Education, Hubei Key Laboratory of Stomatology, School & Hospital of Stomatology, Wuhan University, Wuhan, 430079, China
[b] Department of Oral and Maxillofacial Surgery, School and Hospital of Stomatology, Wuhan University, Wuhan, 430079, China

ARTICLE INFO

Article history:
Received 26 April 2024
Received in revised form
26 June 2024
Accepted 2 September 2024
Available online 3 September 2024

Keywords:
Micro/nanomotor
Imaging
Drug delivery
Urease
Biomedicine

ABSTRACT

Enzyme-powered micro/nanomotors (MNMs) (EMNMs) use natural enzymes to facilitate the decomposition of fuels, including hydrogen peroxide (H_2O_2), glucose, triglycerides, and urea to provide power. EMNMs can achieve self-propulsion through the *in situ* utilization of biofuels without additional fuels, exhibiting excellent biocompatibility and significant potential for application in the biomedical field. Compared with H_2O_2, which may cause oxidative damage to the body, urea exhibits superior biosafety characteristics. Presently, urease-powered MNMs (UMNMs) have made notable progress in their applications in the biomedical field and have garnered considerable attention from researchers. In this review, we present the latest advancements in the biomedical field of UMNMs, primarily focusing on: 1) diverse materials used for constructing the fundamental framework of motors; 2) control of motor movement through the regulation of enzymatic reaction rates; and 3) research directions for the clinical application of motors, including *in vivo* imaging, biomarker detection, cancer treatment, optical therapy, overcoming biological barriers, antibacterial interventions, antithrombotic strategies, and gastric disease management. Despite showing immense potential in biomedical applications, there are still several challenges impeding its practical implementation, such as maintaining activity in the *in vivo* environment while accurately targeting specific sites to achieve the desired clinical therapeutic effects.

1. Introduction

In living organisms, natural biological motors such as myosin and dynein play crucial roles in substance transport, information transfer, and other biological activities within cells by converting chemical energy into mechanical energy [1]. Because of this phenomenon, studies have aimed to develop micro/nano scale devices that can transform different forms of environmental energy (such as chemical [2–4], light [5,6], electric [7,8], magnetic [9,10], and ultrasound [11,12] energies) into mechanical energy to facilitate autonomous movement. Micro/nanomotors (MNMs) are movable devices with specific functions at the micro/nano scale, capable of performing tasks in microscopic environments. Owing to their small size, autonomous propulsion, controllable motion, load capacity, and swarming capabilities, MNMs have extensive applications in diverse areas, including analytical chemistry, drug delivery, precision medicine, biosensing, and environmental remediation [13–15]. The biomedical applications of MNMs, particularly in surgery, diagnosis, and medical imaging, have great potentials for enhancing precision and enabling remote operations [16]. However, significant progress is required before these motors can be effectively used *in vivo*. A major hurdle arises from the restricted biocompatibility and biodegradability of the materials employed to fabricate these motors. Such materials may trigger immune responses or inflammation because they are perceived by the body as latent harmful substances [17].

Enzymes are widely distributed in living organisms and serve as crucial catalysts with significant specificity and catalytic efficiency. These biological catalysts are characterized by excellent biocompatibility and biodegradability, enabling the catalysis of bioavailable substrates such as hydrogen peroxide (H_2O_2), glucose, urea, and fats under mild conditions [18]. The chemical energy stored in biofuels can be efficiently converted into mechanical energy for motor propulsion without the need for additional fuels, making it highly compatible with biological systems. Therefore, biofuels also

* Corresponding author. State Key Laboratory of Oral & Maxillofacial Reconstruction and Regeneration, Key Laboratory of Oral Biomedicine Ministry of Education, Hubei Key Laboratory of Stomatology, School & Hospital of Stomatology, Wuhan University, Wuhan, 430079, China.
** Corresponding author. Department of Oral and Maxillofacial Surgery, School and Hospital of Stomatology, Wuhan University, Wuhan, 430079, China.
E-mail addresses: zili09@whu.edu.cn (Z.-L. Yu), junjia@whu.edu.cn (J. Jia).
Peer review under responsibility of Xi'an Jiaotong University.

https://doi.org/10.1016/j.jpha.2024.101095

show significant potential for widespread applications in biomedical fields. Currently, most chemically propelled MNMs rely on H_2O_2 [19–21]. A clear concentration gradient in the distribution of H_2O_2 exists in cells and tissues in the human body, with intracellular concentration of about 1–100 nM [22] and plasma concentration of about 1–5 μM [23], which is more than 100-fold the intracellular concentration. Excessive H_2O_2 can cause oxidative damage to cells and tissues [24,25]. Although researchers are attempting to devise motors that can operate at lower concentrations of H_2O_2, the required concentration used in the experiments (in millimoles) remains far beyond the normal physiological range [26–28]. In addition, the bubbles produced during the decomposition of H_2O_2 have an adverse effect on the internal environment. Therefore, the use of catalase-powered motors in the biomedical field is limited. Urea, a metabolic by-product in humans, is synthesized in the liver and subsequently transported through the bloodstream for renal excretion as urine. The concentration of urea ranges from 5 to 10 mM in human blood, whereas it can reach as high as 300 mM in urine [29], serving as a fuel source for driving motors. Urease efficiently decomposes urea into ammonia (NH_3) and carbon dioxide (CO_2) in the absence of bubbles, thereby preventing interference from the body's internal environment. Owing to the nontoxic nature of their substrates and products, the potential of urease-powered MNMs (UMNMs) for diverse applications in the biomedical field has attracted considerable attention in recent years.

This article outlines the fundamental structure, motion control, and current research progress of UMNMs in the biomedical field, specifically focusing on disease diagnosis and treatment. Despite significant advancements in UMNMs research, numerous challenges and issues persist throughout the journey from experimental stages to clinical applications, including preserving urease activity within complex bodily fluid environments, effectively regulating motor speed and directionality, and managing motors upon task completion.

2. Materials for frameworks composition

Most framework materials for MNMs exhibits neither biocompatibility nor biodegradability within biological environments, potentially eliciting immune reactions or inflammatory responses, as these entities are identified as foreign by host systems, thereby impeding their effective functioning [30]. To meet the demands of practical applications, scientists have explored the possibility of using materials with good biocompatibility and easily functionalized surfaces for the fabrication of motor systems. This article introduces novel materials that have attracted widespread attention, including different organic or inorganic nanoparticles (NPs) (such as metal-organic frameworks (MOFs), silica NPs, and polydopamine (PDA) NPs), liposomes, and biological components (such as platelets, neutrophils (NEs), and human serum albumin (HSA)).

2.1. NPs

NPs have diameters ranging from 1 to 100 nm, composed of metals, mental oxides, organic matter, and carbon [31]. These NPs exhibit unique physical and chemical characteristics, including ultrasmall and controllable size, large surface area, and the capacity to easily modify and functionalize the surface [32]. These features contribute substantially to the preparation and optimization of MNMs, conferring great advantages in improving disease diagnosis, treatment, and targeted drug delivery. The following discussion will primarily focus on several emerging materials with promising applications while introducing their characteristics as frameworks for MNMs.

2.1.1. MOFs

MOFs are a crystalline material class composed of metal ions or clusters and organic ligands, with robust highly ordered porous three dimensional (3D) structures, providing significant potential for numerous applications, including catalysis [33,34] and drug delivery [35,36], which may serve as effective candidate materials for improving the stability and efficiency of MNMs [37–39]. Compared to traditional MNMs, MOF-based MNMs (MOFtors) have several advantages, such as simple production processes, large specific surface areas, structural stability, and low toxicity. Because of these benefits, MOFs have emerged as a significant alternative approach for addressing challenges within the MNMs field [40]. Currently, MOFtors are primarily employed in biomedicine to encapsulate, regulate the release and deliver targeted amounts of biological agents [41–43]. A dual enzyme-modified nanomotor based on zeolitic imidazolate framework-8 (ZIF-8, a kind of MOFs) was reported (Fig. 1A) [44]. Owing to the porosity of ZIF-8, enzymes, upconversion NPs (UCNPs), and hydrophobic photosensitizers can form nanomotors stably, showing the anti-cancer effect of synergistic treatment.

The movement and function of UMNMs depend on urease activity; however, urease activity is reduced or absent in harsh environments (such as high temperatures and strong acids). To address this issue, Liang et al. [45] reported the initial study of biomimetic mineralization of MOFs. In this process, biomacromolecules encapsulate themselves within the porous crystal and control the formation of crystals. This method preserves the functionality of biomacromolecules, such as proteins and enzymes, against harsh situations. The controlled release of biomacromolecules from protective MOF coatings can be accomplished through pH modifications, providing a new approach for protecting and delivering bioactive substances. However, this protective barrier, which impedes molecular transport, may lead to reduced enzyme catalytic efficiency, thereby affecting motor mobility. Therefore, Kim and coworkers [46] proposed a flow synthesis method. The results indicate that compared to crystalline nanomotors, the amorphous ZIF-8 nanomotor (A-motor) provides effective protection for enzymes without sacrificing molecular transport. The A-motor exhibits satisfactory biocompatibility and good augmented motions in a urea-containing basic aqueous environment (pH 9.5). Therefore, MOFs are available materials for the synthesis of MNMs, and serial flow-assisted synthesis, as an effective method to improve material performance, is worthy of further exploration.

2.1.2. Mesoporous silica NPs (MSNPs)

Among the various inorganic nanomaterials, MSNPs have received a wide range of concerns from researchers owing to their highly organized pore structure, adjustable pore size and shape, simple surface functionalization, and excellent chemical stability [47,48]. These superior physical and chemical properties make them ideal platforms for various biomedical applications and are extensively used in the preparation of MNMs [2,4,49–51].

As multifunctional carrier platforms, MSNPs can load various cargoes (such as drugs and biomacromolecules) and exhibit good biocompatibility. Researchers have developed UMNMs using MSNPs and incorporated antibodies, anticancer drugs, and antibacterial drugs [52–55]. Their work illustrated that active motion can augment the targeting precision and drug delivery efficacy of motors. Furthermore, it validated the feasibility and practicality of employing MSNPs as scaffolds for motor fabrication (Fig. 1B) [55]. To prevent drug leakage and control release of the active ingredient, researchers have blocked the pores of MSNPs with phenyl imidazole-cyclodextrin-urease caps to achieve pH-responsive drug release [56].

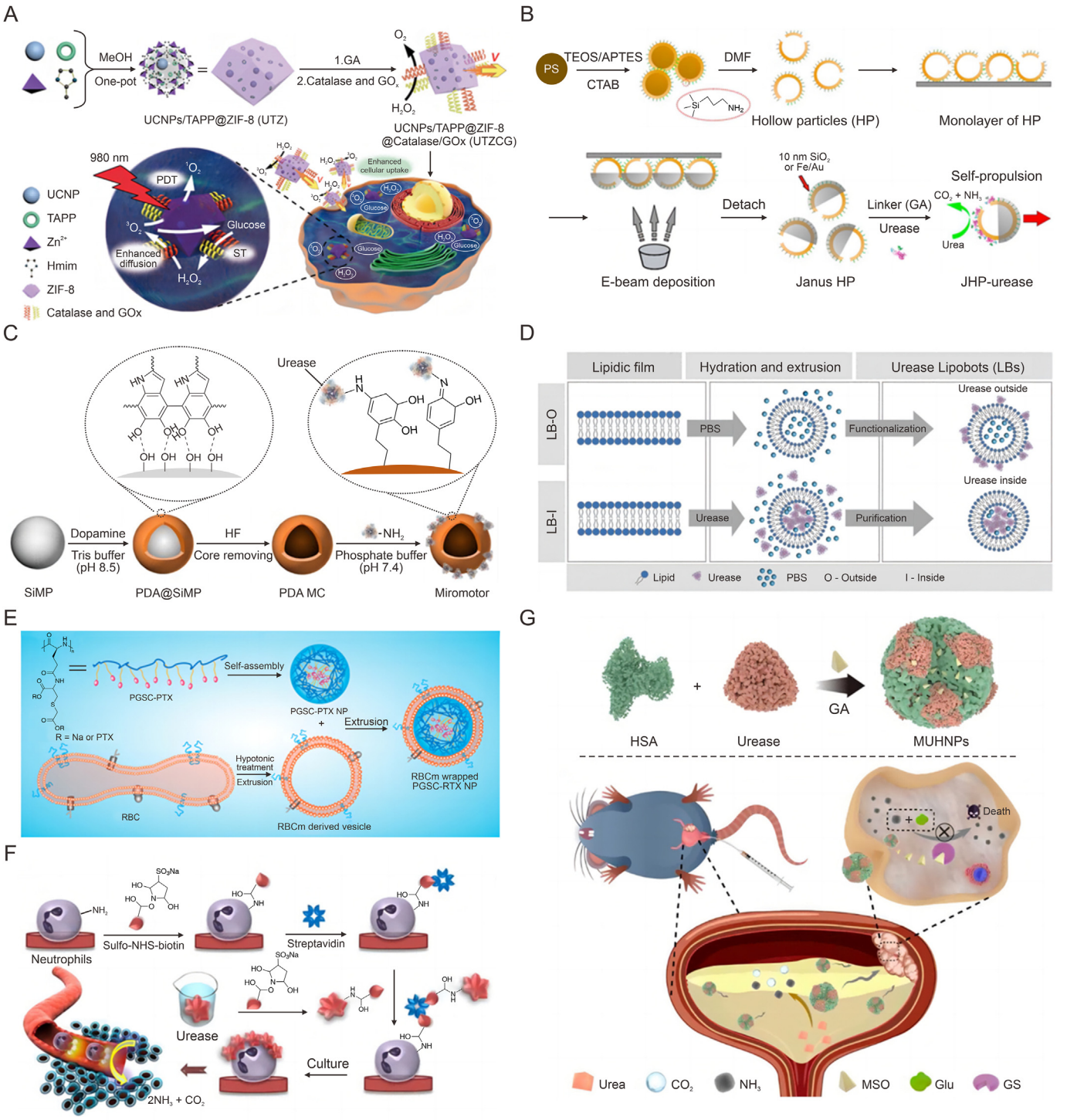

Fig. 1. Schematic diagram of the preparation of micro/nanomotors (MNMs) by different materials. (A) The fabrication of nanomotors based on metal-organic framework (MOF) nanoparticles (NPs) [44]. (B) The fabrication of microcapsule (MC) motor based on Janus hollow mesoporous silica microparticles [55]. (C) The preparation procedure of urease-powered polydopamine (PDA) micromotors [62]. (D) The fabrication process of Lipobots-Outside (LB-O) and Lipobots-Inside (LB-I) [67]. (E) Schematic diagram of the preparation process of the poly(L-γ-glutamylcarbocistein) (PGSC)-paclitaxel (PTX)@red blood cell membrane (RBCm) NPs [74]. (F) Synthetic route of urease catalysis micromotor-powered neutrophils (NEs) [78]. (G) Synthetic procedure of L-methionine sulfoximine (MSO)-loaded urease-driven human serum albumin (HSA) NPs (MUHNPs) [82]. UCNP: upconversion NP; TAPP: 5,10,15,20-tetrakis(4-aminophenyl)porphyrin; ZIF-8: zeolitic imidazolate framework-8; GOx: glucose oxidase; GA: glutaraldehyde; PDT: photodynamic therapy; ST: starvation therapy; Hmim: 2-methylimidazole; PS: polystyrene; TEOS: tetraethylorthosilicate; APTES: 3-aminopropyltriethoxysilane; CTAB: cetyltrimethylammonoium bromide; DMF: dimethylformamide; MP:microparticle; Glu: glutamate; GS: glutamine synthetase. Reprinted from Refs. [44,55,62,67,74,78,82] with permission.

The morphological traits and physical and chemical properties of MSNPs can be significantly enhanced through advanced surface modifications (employing polymers, liposomes, biological membranes, and protein coatings), silica skeleton alterations (integrating organic components and metal substances), and meticulous pore structure adjustments (including cage-like, hollow, eggshell, and core-shell configurations). These interventions not only enrich the mesoporous architecture but also amplify its

multifunctionality [57]. In the biomedical field, MSNPs hold promise for further exploration as drug carriers, imaging agents, and biosensors, owing to their customizable and versatile properties.

2.1.3. PDA NPs and coatings

Reflection on nature can lead to unexpected rewards. Through long-term observations and research on mussels, Harrington and co-workers [58] found that 3,4-dihydroxyphenylalanine (DOPA) and proteins rich in lysine are key substances for their adhesion. Based on this, scientists have found that PDA, with a DOPA-like molecular structure, exhibits several properties strongly linked to its chemical structure and composition, including biocompatibility, strong photothermal conversion ability, high adhesion, and chemical reactivity [59,60].

PDA NPs of different sizes can be synthesized by adjusting reaction conditions. Owing to their adsorption capacity and active functional groups on the surface, PDA NPs can be assembled into shells with various polymers and functional substances as coating materials to meet specific needs. For example, covalently coupling HSA to the surface of PDA NPs improves nanomotors dispersion and stability [61]. The high adhesion of PDA can also prolong its residence time in the body and improve the permeability of molecules as oral drug carriers in the stomach (Fig. 1C) [62]. Furthermore, PDA can absorb near-infrared (NIR) light effectively and transform it to heat energy, making it ideal for photothermal applications with significant advantages in photothermal therapy (PTT) [46]. PDA is easy to surface modify, allowing it can combine PTT with other treatments to inhibit tumor proliferation [61]. At the same time, the strong adhesion enables PDA can adhere to surfaces of organic and inorganic materials. Therefore, PDA can help to improve the solubility and stability of materials and serve as a connector to introduce various functional molecules onto material surfaces.

2.1.4. Liposomes

Since the concept of liposomes was first introduced [63,64], these lipid-based vesicles have been the subject of extensive research as delivery carriers for various needed molecules. Owing to the fundamental similarity of the liposomal structure to biological membranes, which also comprise phospholipid bilayers, liposomes are considered to have good biocompatibility and biodegradability [65]. In addition, liposomes are easy to prepare and modify, and lipid NPs (LNPs) developed on this basis can control the delivery location and time of drugs in the body, making them possible to treat different diseases [66].

The structure similar to that of cell membranes allows liposomes to protect drugs from enzymatic degradation before reaching the destination. For instance, Sánchez and co-workers [67] designed two types of liposomal UMNMs, namely LipBots (Fig. 1D) and studied the functional features of LipBots, including their capacity to withstand acidic environments and their demand-driven activation. The result showed that sodium deoxycholate disrupts and permeabilizes the lipid bilayer, acting as an edge activator. In addition, following a 1 h incubation period in acidic circumstances, the lipid bilayer surrounding the encapsulation protects the encapsulated urease LipBots from harsh conditions, allowing them to regain activity and motility, while the urease attached to the surface loses both. These findings pave the way for the use of LipBots as active drug delivery devices in a variety of *in vivo* settings. The surface modification of liposomes through physicochemical means can confer tissue targeting, prolong effective retention at the disease site, and achieve efficient targeted drug delivery [68−70]. Drugs encapsulation within liposomes enhances their stability, reduces toxicity, increases dosage, and improves therapeutic efficacy.

2.2. Natural origin

Synthetic nanomaterials, whether organic or inorganic, have drawbacks include difficult preparation procedures and vulnerability to immune system identification and removal. Considering the feasibility of applying nanomotors *in vivo*, recent researches have focused on biomimetic nano delivery systems constructed using living cells as carriers or employing bio-membrane-coated modified nanocarriers. These systems exhibit good biocompatibility and low immunogenicity and have attracted widespread attention from researchers.

Natural cells [71] and cell membranes [72] can directly confer various biological functions to nanocarriers without requiring intricate synthetic designs. For example, red blood cells (RBCs) [73], which are abundant in blood and can circulate for up to 120 d, lack a cell nucleus and various organelles, making RBC membranes easy to extract and purify. Using RBC membranes to coat drug delivery carriers enhances the circulation time of nanodrugs in the bloodstream and immune evasion (Fig. 1E) [74]. Wang and co-workers [75] developed a Janus platelet micromotor (JPL-motor) system through asymmetric immobilization of urease on the natural platelet surface. This system exhibits inherent platelet characteristics and self-propulsion; exhibits good biocompatibility, transportability, and targeting capabilities; and is applicable to various cell types and enzymes. This forges the path for a new approach for the clinical application of nanomotors. Immune cells play a role in protecting the body from infections, attacking foreign invaders, and fixing damaged tissues. Leveraging these cells for biomimetic design allows the targeted treatment of inflammatory or tumor sites [76,77]. Sang and co-workers [78] exploited the targeting characteristics of NEs to inflammatory sites to fabricate urease micromotor powered Janus NEs (UM-NEs) (Fig. 1F). Urease-catalyzed endogenous urea actively propels NEs toward thrombus sites, in which the abundant inflammatory cytokines can activate NEs to form NE extracellular traps (NETs), releasing silver (Ag)-urokinase (UK), causing thrombus dissolution and vascular recanalization.

Albumin, with the highest plasma (35−50 mg/mL), can transport endogenous or exogenous hydrophobic molecules [79]. HSA, a major type of albumin, is a suitable drug carrier because of its biocompatibility, biodegradability, nonimmunogenicity, and high binding capacity [80,81]. Tu and co-workers [82] crosslinked urease with HSA to prepare L-methionine sulfoximine (MSO)-loaded urease-driven HSA NPs (MUHNPs) (Fig. 1G). The motors achieved adhesion and retention in the bladder and effectively killed tumor cells by leveraging the toxic effects of NH_3, which were amplified by MSO. HSA NPs can also be used to modify the motor surface to enhance biocompatibility and extend circulation time in the body [83].

However, problems remain to be solved to truly apply biomimetic drug delivery systems in the clinic: immature cell extraction and purification methods, and difficulties ensuring the integrity of bioactive components (including ion channels, enzymes, and receptors) on cell membranes during the preparation process. Despite these challenges, the future prospects are promising, motivating researchers to continue exploring.

3. Motion control of UMNMs

The essence of enzyme-powered MNMs (EMNMs) are catalytic reactions. Therefore, changes in the catalytic speed of enzymes can be used to regulate motor motion by adjusting the substrate concentration, enzyme activity, and quantity and distribution of enzymes. The design of the motor structure can also influence its driving performance, motion speed, and trajectory. In addition,

real-time control of motor motion can be achieved by coupling external field-responsive materials and combining them with other driving modes (such as light [61], sound, and magnetic fields [55,84]).

3.1. The concentration of the substrate

As the energy source for motor motion, changing the substrate (urea) concentration can effectively control the catalytic speed, thereby regulating the motor's motion speed [55,84] and diffusion behavior [4,52]. The motor motion velocity changing with the substrate concentration trend was similar to that of Michaelis-Menten enzyme kinetics. An rise in the substrate concentration causes the reaction rate to speed up, the energy converting efficiency to improve, and the UMNMs to move more easily within a certain concentration range. Once the concentration of the substrate surpassed a specific threshold, the rate of the reaction ceased to escalate, and the movement of the motor entered a plateau stage (Fig. 2A) [55]. Furthermore, the correlation between the movement of UMNMs and the substrate concentration enabled them to exhibit chemotaxis, similar to that of enzymes, across substrate concentration gradients. Urease exhibits positive chemotaxis across its substrate gradient [85], as does urease-coated solid particles. For instance, urease-driven polystyrene (PS) particles exhibit positive chemotaxis by migrating toward regions with higher urea concentrations in the substrate concentration gradient [86]. However, Somasundar et al. [87] discovered that urease-driven liposome motors exhibit negative chemotaxis, migrating toward areas of lower substrate concentration, potentially as a result of solute-phospholipid interactions. The ability to exhibit directed movement along substrate concentration gradients endows artificially synthesized EMNMs with considerable potential for applications like delivering drugs.

3.2. The activity of enzymes

Enzyme activity, a key factor in catalytic reactions, directly affects the self-propulsion force of enzyme-driven motors. The regulation of enzyme activity allows the manipulation of the velocity of these motors. The inhibition of urease activity by Ag and mercury (Hg) is mediated by the formation of urease-inhibitor complexes [88]. Thiol protectants, like dithiothreitol (DTT), competitively bind to create DTT-inhibitor complexes, which restore urease function and reverse the reversible inhibitory process [89]. Sánchez and co-workers [55] added inhibitors (Ag or Hg) into a urea-containing solution and observed a gradual decrease in motor speed as the concentration of the inhibitor increases. When the concentration reached 0.5 μM, the motor completely ceased its directional movement. However, the enzyme was rapidly reactivated upon the addition of DTT, and triggered immediate motor movement. These findings illustrate that the enzymatic reaction fuels the self-propulsion mechanism and is contingent on enzyme activity levels.

To gain a more profound understanding of the effect of intrinsic enzymatic characteristics, they employed a combination of experimental techniques and molecular dynamics simulations to investigate [50]. These results indicate that urease and acetylcholinesterase, which are characterized by higher catalytic rates, possess the ability to drive the motor system effectively, resulting in significant movement. Moreover, they exhibited enhanced flexibility around the active site compared to glucose oxidase and aldolase. The role of structural flexibility was investigated by changing the rigidity around the urease active site. A decrease in motor speed was observed, indicating that reducing the flexibility would impact its catalytic activity and diminish the self-propulsion force of the motor (Fig. 2B) [50].

Enzyme activity is also influenced by the purity of the protein, and the current commercial ureases used for motor movement are impure. Valles et al. [90] have conducted a comparison between purified and unpurified UMNMs, revealing that purified UMNMs have an average speed of 5.5 μm/s, which is 2.5-fold faster than unpurified ones, indicating superior movement performance and higher reusability (Fig. 2C).

3.3. The quantity and spatial distribution of enzymes on MNMs

The number and spatial distribution of enzymes in the motor surface are common ways of regulating motor behavior. In general, the propulsion force of EMNMs is weak, which significantly limits their application in complex biological environments. As the enzyme load increased, the motor movement was enhanced, as shown by Luo et al. [91], who assembled biotinylated urease (BU) in multiple layers using streptavidin (SA) as a crosslinker and immobilized it asymmetrically on magnetic microparticles. As the surface urease load increased, the propulsive force of the motor increased significantly (Fig. 2D). In 10 mM urea aqueous solution, the average velocity of the multi-layer urease-driven motor reached 21.5 ± 0.8 μm/s, which was 5-fold faster than that of the single-layer motor. Therefore, constructing MNM motors with multiple layers of urease is an effective approach for increasing the enzyme load and improving motor motility. By comparing PS and PS@SiO_2 motors, Sánchez and co-workers [3] found that even when urease showed a similar uneven distribution on both surfaces, the PS@SiO_2 micromotor surface could bind more urease than PS, resulting in better self-propulsion.

Even the same amount of enzymes were loaded, the enzyme spatial distribution on the motor significantly affected the motor performance of the EMNMs. Wang and co-workers [75] prepared JPL and non-JPL motors by asymmetrically immobilizing and uniformly anchoring urease onto the surface of platelet micromotors. At a urea concentration of 200 mM, the movement speed of the JPL motor was 1.62-fold higher than that of the non-JPL motor. Because enzymes distributed unevenly on the surface, the JPL motor exhibited superior motor performance and more pronounced diffusion behavior (Fig. 2E). Similarly, Guan and co-workers [92] fabricated ultrasmall urease-powered Janus nanomotors (UPJNMs) using gold NPs as the carrier, modifying one side with polyethylene glycol (PEG), and immobilizing urease on the other side (Fig. 2F). They compared this with non-UPJNMs where urease was uniformly fixed on the surface, and showed that the Janus structure conferred significant self-propulsion and enhanced chemotaxis to the motor. Ma et al. [84] developed silica nanotube-based motors for the selective immobilization of urease on the surface or throughout the structure of the nanotubes. Motors with internal or complete immobilization of urease illustrate longitudinal self-propulsion, in contrast to those with externally immobilized urease, which exhibit only Brownian motion. These findings present a novel propulsion mechanism for tubular motors that the motor movement can be attributed to the active flow generated by the enzymatic reaction products.

3.4. The design of motor structure

The structure, size, surface properties, and other factors of the motor can significantly affect the movement behavior of EMNMs. A well-designed structure has the potential to enhance the motion of EMNMs. For example, van Hest and co-workers [93] developed a gourd-shaped nanomotor using aggregation-induced emission (AIE) aggregates (Fig. 2G). The asymmetry achieved through this unique structure, combined with the inhomogeneous urease modification on the surface, enables self-propulsion. This

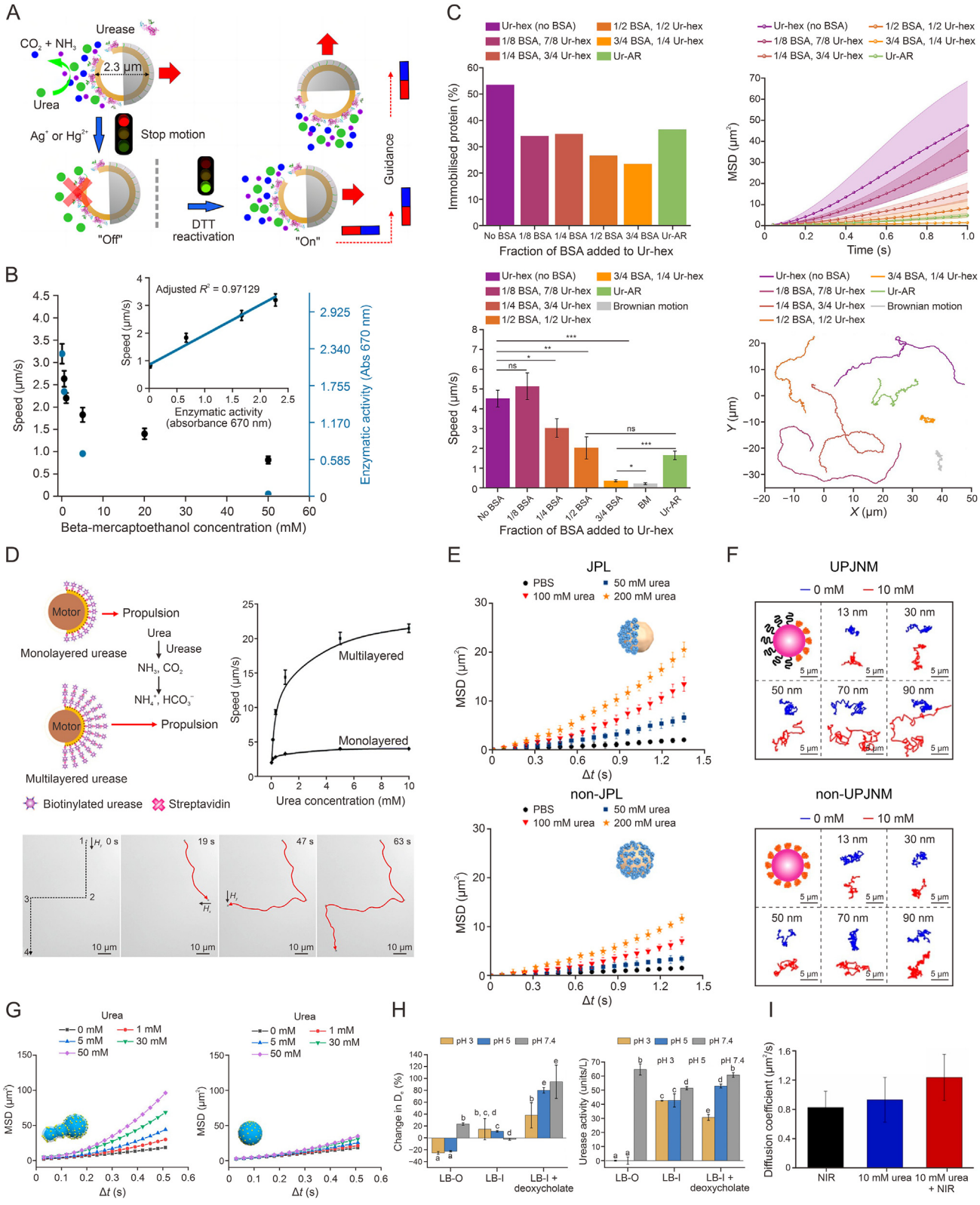

Fig. 2. Motion control of urease-powered micro/nanomotors (MNMs) (UMNMs). (A) Motion control of the urease-powered microcapsule motor by chemical addition and magnetic fields [55]. (B) Effect of enzyme intrinsic properties on self-propulsion [50]. (C) Mobility of urease micromotors influenced by protein impurities [90]. The *P* values determined from pairwise *t*-tests are represented in the NEJM format: $^{*}P \leq 0.05$, $^{**}P \leq 0.01$, and $^{***}P \leq 0.001$. ns: not significant. (D) Enhanced propulsion of the multilayered UMNMs based on Janus magnetic microparticles [91]. (E) Motion behavior of Janus platelet micromotors (JPL-motors) and urease fully modified platelets (non-JPLs) [75]. (F) Motion behavior of the ultrasmall urease-powered Janus nanomotors (UPJNMs) and non-UPJNMs of varied sizes. Blue trajectory represents the motion of the motor in 0mM urea aqueous solution, and red trajectory represents the motion of the motor in 10mM urea aqueous solution. [92]. (G) Characterization and motion behavior of fluorescent polymersome-based enzyme-driven aggregation-induced emission-nanomotors [93]. (H) The protective effect of the lipid shell on the urease in acidic conditions and recovery of the motion capabilities of Lipobots. Results are shown as mean ± standard error of the mean (SEM), left panel: $n = 5$; right panel: $n = 3$. Different superscript letters (a–e) indicate significant differences ($P < 0.05$);

asymmetric scaffold provides a novel approach for improving motor performance. In addition, the characteristics of the motor surface are important in determining the microenvironment needed for the enzymatic catalytic processes. These properties not only influence the conformation and activity of immobilized enzymes but also affect fuel molecule-enzyme interactions. Therefore, modifying the motor surface properties allows the regulation of enzyme catalytic activity and subsequently influences EMNM movement. Sánchez and co-workers [67] employed liposomes as the structural framework of UMNMs while encapsulating urease to shield them from harsh environmental conditions (Fig. 2H). Upon reaching the target site, sodium deoxycholate was introduced to modulate lipid bilayer fluidity, effectively regulating substrate-urease interactions and subsequently controlling motor behavior.

3.5. Combination of multiple driving modes

The incorporation of external field-responsive materials and UMNMs facilitates the implementation of diverse driving modes, including light [61] and magnetic fields [55,91], for the real-time control of motor movement. For example, the incorporation of photothermal materials during motor preparation can regulate the local environmental temperature through external light, thereby controlling the catalytic performance of the enzyme to achieve precise control over motor movement. Wu et al. [61] achieved the photo-response motion by coupling the photosensitive material PDA with UMNMs (Fig. 2I). The experiment showed the feasibility of using NIR laser to enhance the catalytic activity and the motion of PDA nanomotor. Ma et al. [55] successfully manipulated the movement direction by integrating magnetic materials onto the motor surface and applying a magnetic field. Similarly, urease motors fabricated using magnetic microparticles exhibit significant responsiveness to magnetic fields and can navigate along specific routes under external guidance signals [91]. This combined regulatory approach provides a crucial foundation for future *in vivo* targeted therapies.

3.6. Models used to predict the motion of MNMs

To promote the biomedical application of MNMs, real-time trajectory prediction and control over their movement are also important. The movement of EMNMs is primarily driven by the asymmetric distribution of substrates and products, and there are four main mechanisms: bubble recoil propulsion [94], self-diffusiophoresis [95], self-electrophoresis [96], and the interfacial tension gradient [97,98].

The asymmetric enzyme distribution around the UMNMs surface can cause a concentration gradient in the charged material, which causes the UMNMs to rely on self-electrophoresis for autonomous movement [84]. Because the motion depends on a complicated interaction at the surface-fluid interface of the motor and is strongly influenced by Brownian motion, chemically propelled MNMs suffer from great uncertainty regarding their trajectory. To solve this problem, researchers have designed magnetic components to be added to motors to achieve directional control [55,99]. By collecting and analyzing previous experimental data, Folio et al. [100] developed an appropriate model using the state-dependent coefficient (SDC) with dual Kalman filter (DKF) algorithm to study the motion behavior of a magnetic Janus microrobot (MJR) propelled by a self-phoresis mechanism, and showed that the SDC-DKF can be used to predict the behavior of magnetic Janus catalytic microrobots, even if the inputs are unrecognized. However, this model fails to describe magnetic Janus micromotors (MJMs) with disparate magnetic moments or those propelled by mechanisms based on bubble recoil. Therefore, a dynamic model, SDC robust two-stage Kalman filter (SDC-RTSKF), was developed to accurately depicts the MJMs of these conditions [101]. MJMs were fabricated by depositing Co/Pt bilayers with different thicknesses onto self-assembled monolayers of SiO_2 microspheres. By adding surfactants to the H_2O_2 fuel solutions, they observed the movement of MJMs propelled by the bubble recoil mechanism. They found that the system dynamics of a magnetic Janus catalytic micromotor can be estimated through an SDC-RTSKF. The experiments showed good match between theoretical forecasts and experimental observations in both studies. These proposed models pave the way for more precise and advanced motion control and can be extended to various MNMs that contribute to the development of MNMs for biomedical applications.

4. Application of UMNMs in the field of disease detection and diagnosis

4.1. Imaging agents

Using imaging examinations to acquire anatomical structures and physiological data of patients enables clinicians to comprehensively understand the occurrence and progression of diseases, facilitate accurate diagnosis, and develop appropriate treatment plans. UMNMs possess excellent biocompatibility and autonomous mobility, making them suitable imaging agents for enhancing the precision of medical imaging technologies. The application of MNMS in *in vivo* imaging has been extensively studied.

4.1.1. Radionuclide

The combination of positron emission tomography (PET), with computed tomography (CT) for tracking radiolabeled MNMs allows for improved visualization and control of NP populations, thereby facilitating their translation into clinical applications [102]. Sánchez and co-workers [2] radiolabeled UMNMs with either ^{124}I on gold NPs or ^{18}F-labeled prosthetic group to urease, and validated the swarming behavior of these enzyme nanomotors through medical imaging techniques (Fig. 3A). The injected motors exhibited enhanced liquid-mixing ability within the bladder, while being uniformly distributed throughout the bladder. Moreover, direct radionuclide labeling of enzymes has proven to be a stable method for imaging purposes, PET-CT is also an appropriate technique for visualizing nanomotors.

4.1.2. Liquid metals

Liquid metals include post-transition metals, zinc-group metals (excluding zinc), and their alloys. Owing to their low melting points (below 300 °C) and their unique combination of metallic and liquid

groups with the same letter are not significantly different. In left panel, a: No significant difference between LB-O groups at pH 3 and pH 5. b: No significant difference among LB-O group at pH 7.4, LB-I group at pH 3, and LB-I in the presence of 0.075% sodium deoxycholate group at pH 3. c: No significant difference between LB-I groups at pH 3 and pH 5. d: No significant difference between LB-I groups at pH 3 and pH 7.4. e: No significant difference between LB-I in the presence of 0.075% sodium deoxycholate groups at pH 5 and pH 7.4. In right panel, a: No significant difference between LB-O groups at pH 3 and pH 5. b: No significant difference between LB-O group at pH 7.4 and LB-I in the presence of 0.075% sodium deoxycholate group at pH 7.4. c: No significant difference between LB-I groups at pH 3 and pH 5. d: No significant difference between LB-I group at pH 7.4 and LB-I in the presence of 0.075% sodium deoxycholate group at pH 5. e: Significant difference between LB-I in the presence of 0.075% sodium deoxycholate group at pH 3 and all other groups [67]. (I) Diffusion coefficient values of UMNMs in different conditions [61]. DTT: dithiothreitol; MSD: mean square displacement; LB-O: Lipobots-Outside; LB-I: Lipobots-Inside; NIR: near-infrared. Reprinted from Refs. [50,55,61,67,75,90–93] with permission.

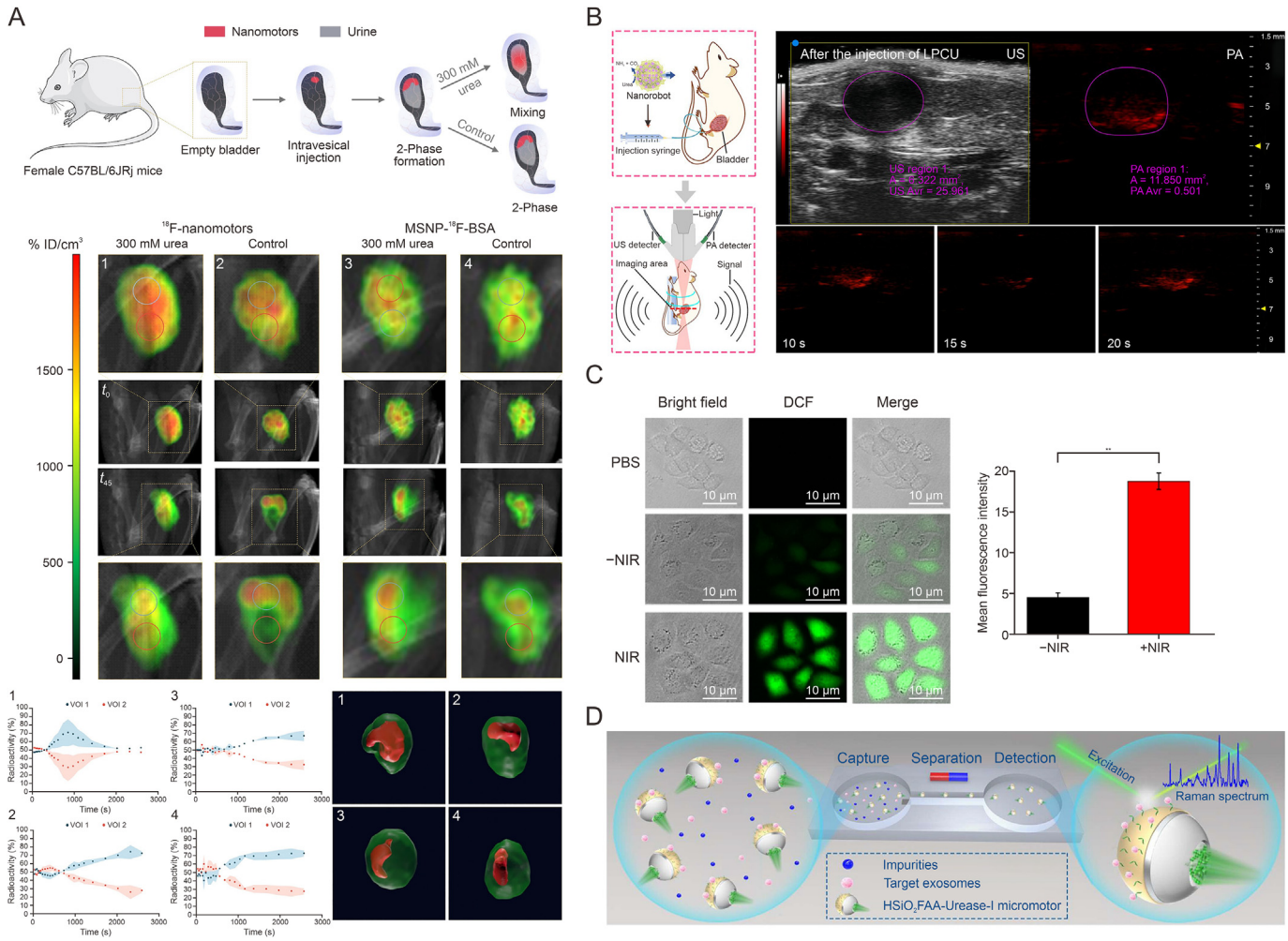

Fig. 3. Urease-powered micro/nanomotors (MNMs) (UMNMs) for disease detection and diagnosis. (A) Urease-powered nanomotors swarming behavior by positron emission tomography (PET) in combination with computed tomography (CT) (PET-CT) imaging techniques [2]. (B) Ultrasonic (US) and photoacoustic (PA) images of urease-powered liquid metal (LM) nanobots [109]. (C) Urease-powered human serum albumin (HSA) nanomotor for fluorescence imaging [83]. The Student's *t*-test was applied to analyze the difference between different treatment groups. Significant differences were considered at $P < 0.05$ and expressed as $^{**}P < 0.01$. (D) Exosomes capture and detection using urease-powered micromotors [118]. MSNP: mesoporous silica nanoparticle (NP); BSA: bovine serum albumin; VOI: volumes of interest; LPCU: LM@polydopamine (PDA)@cefixime trihydrate (CF) and Urease; PBS: phosphate-buffered saline; NIR: near-infrared; $HSiO_2FAA$-Urease-I: hollow multilayered SiO_2 ($HSiO_2$)@Fe@Au-aptamer-linked-Urease inside micromotors. Reprinted from Refs. [2,83,109,118] with permission.

properties, these materials exhibit exceptional capabilities in synthesis, catalysis, sensing, and therapy [103,104]. Among the various liquid metals, gallium (Ga) and its alloys have garnered significant attention owing to their beneficial features, including biodegradability, low toxicity, and convertibility [105,106]. Although metal compounds are commonly employed as contrast agents, the detachment of metal ions from chelating agents can potentially cause varying degrees of organ damage, including damage to the kidneys, liver, and brain. By contrast, GA-based modified materials exhibit exceptional biocompatibility and biodegradability, rendering them suitable for applications in X-ray imaging, CT scans, and photoacoustic imaging [107,108]. Notably, Ma and co-workers [109] successfully developed urease-powered liquid metal (LM) nanomotors based on a Ga-In-Sn alloy (Fig. 3B). The LMs showed notable imaging properties using both ultrasound and photoacoustic techniques, enabling the successful visualization of the movement of MNM motors within the urinary bladder of live mice.

4.1.3. Fluorescence imaging

Currently, all imaging techniques used in clinical practice have their own advantages and limitations. For instance, magnetic resonance imaging (MRI) exhibits exceptional visualization of soft tissue lesions; however, the use of gadolinium-based contrast agents may pose risks to patient well-being. Moreover, CT has low sensitivity and relies on ionizing radiation. Compared to conventional imaging modalities, fluorescence imaging has numerous advantages, including high sensitivity, selectivity, non-invasiveness, real-time capability, field responsiveness, and simplicity of application [110]. Fluorescent agents have been intensively investigated as the cornerstone of fluorescence imaging owing to their exact molecular structure, manageable biocompatibility, adjustable spectral properties, and diverse modification strategies. Consequently, organic dyes and NPs have attracted significant attention in this field [83,93].

Indocyanine green (ICG), an *in vivo* dye with excellent fluorescence stability and low toxicity, is widely used in medical diagnosis and other domains. Shuai and co-workers [83] achieved the real-time tracking of cell movement by incorporating ICG into the motor system (Fig. 3C). Interestingly, ICG also exhibited efficient photothermal conversion ability upon NIR light irradiation, which not only enhanced urease catalytic activity and self-propulsion ability, but also generated abundant reactive oxygen species (ROS) for tumor cell eradication, resulting in superior anti-tumor effect.

New discoveries in one field can provide fresh impetus for the advancement in other fields. With the evolution of AIE, scientists have discovered that AIE luminescent agents (AIEgens) and their NPs formed by them possess notable attributes such as high luminosity, excellent biocompatibility, robust photostability, and a positive correlation between luminescence and concentration [111]. Serving as a direct visualization tool for biological structures and processes, AIEgens and NPs exhibit immense potential in medical imaging and precision medicine as direct visualization tools for biological structures and processes. Cao et al. [93] successfully engineered an AIE-based urease motor that possessed self-propulsion capabilities and favorable biocompatibility through motion behavior tracking analysis and cytotoxicity assays. This study highlighted the feasibility of using materials with AIE properties for nanomotor fabrication and *in vivo* imaging. Furthermore, it has been observed during research advancements that certain AIEgens can serve as efficient photosensitizers in PDT by generating ROS to selectively eliminate cancer cells and pathogens under light irradiation [111].

4.2. The detection of biomarkers

In the early stages of diseases, particularly cancer, accurate diagnosis is often challenging because of the limited sensitivity and specificity of detection methods. This delay in diagnosis can result in postponement of treatment. The identification and detection of relevant biomarkers, such as DNA, proteins, and tumor cells, play a crucial role in achieving early disease detection and have an important impact on the progress of appropriate treatment strategies. One of the key challenges in this field is the utilization of motors to effectively identify and detect biomarkers.

Exosomes are secreted by living cells and widely distributed in bodily fluids. They are small vesicles enclosed by lipid bilayers with diameters ranging from 40 to 160 nm, and belong to a specific type of extracellular vesicles [112,113]. Exosomes, which contain abundant proteins, nucleic acids, and lipids, offer unique insights into diseases and serve as noninvasive cancer biomarkers [114–117]. However, exosome isolation and identification provide substantial obstacles to future study and use. Utilization of the movement properties of MNMs presents a hopeful approach for the isolation and detection of exosomes. Ma and co-workers [118] developed MNMs with urease selectively distributed on the surfaces of hollow particles, enabling the quantitative measurement of the capture efficiency of passive micromotors and inner/outer surface micromotors (46.1%, 63%, and 80.7%, respectively) (Fig. 3D). Their findings indicated that the active movement facilitated by micromotors enhances the likelihood of contact with exosomes, while minimizing the impact exerted by flow fields generated through catalytic reactions on the binding between motors and exosomes when urease is distributed on their inner surfaces. This study exhibited the capability of MNMs to actively move, capture, and detect exosomes, providing a viable strategy for detecting cancer-related markers in a rapid and sensitive clinical setting.

5. The research progress of UMNMs in disease treatment

Precisely targeting drugs to specific sites in the body to improve therapeutic efficacy while reducing side effects on healthy tissues or cells is a great challenge in drug delivery. Traditional drug delivery systems have limitations, such as poor tissue permeability and limited targeting ability [119]. Advancements in modern medicine have necessitated the improvement of novel drug delivery systems that can enhance drug enrichment and penetration at the site of injury. Previous studies showed that MNMs have broad applications. They can transport therapeutic payloads directly to disease sites to minimize the adverse effects on organisms and augment therapeutic outcomes. MNMs can improve cellular uptake and overcome physiological barriers through autonomous movement to augment their therapeutic effectiveness. By modifying the motor function based on the microenvironment of different lesions, targeted delivery can be achieved, ultimately improving drug delivery efficiency. Owing to their excellent biocompatibility and utilization of endogenous fuels in the human body, EMNMs have significant application prospects in drug delivery for multiple diseases.

5.1. Bladder tumor

Bladder cancer is the ninth most common cancer globally. The current clinical treatment includes tumor resection and intravesical chemotherapy [120]. However, owing to the limited drug residence time, low urothelial permeability, and drug susceptibility to degradation in the bladder, frequent drug injections are often necessary. This practice increases the risk of infection and inflammatory reactions, and complicates bladder disease treatment [121]. Consequently, addressing drug permeability and retention in the bladder wall is crucial to developing innovations to treat bladder diseases. Urine urea levels can reach 300 mM [29] and provide ample endogenous fuel for the sustained voluntary movement of UMNMs.

Based on this premise, researchers have focused on UMNMs as evidenced by numerous domestic and international studies. Sánchez and co-workers [52] successfully synthesized UMNMs, which exhibited the ability to load doxorubicin (DOX) and exhibited an enhanced drug release curve dependent on the urea concentration (Fig. 4A). After 6 h exposed to urea, the UMNMs released 4-fold more DOX than the passive NPs. Moreover, the efficiency of the motor in killing tumor cells increased owing to the synergistic effect of NH_3 generated from urea breakdown and the improved kinetics of drug release. Subsequently, they modified the motor by incorporating an anti-fibroblast growth factor receptor 3 (FGFR3) antibody on its outer surface for a specific interaction with the FGFR3 transmembrane protein overexpressed in bladder cancer cells (Fig. 4B) [53]. The results indicated that at equivalent urea concentrations, the antibody-modified motor exhibited heightened cytotoxicity and internalization efficiency compared to the unmodified nanomotor. This enhanced capability facilitated targeted drug delivery. Furthermore, the interaction between the antibody and FGFR3 suppresses the fibroblast growth factor signaling pathway. This further augmented the antitumor efficacy of the motor. During routine drug administration, uncontrolled drug release can lead to drug leakage, which often results in severe toxic side effects. To achieve precise control over drug delivery, researchers introduced benzimidazole groups onto the outer surface of a motor and used benzimidazole and cyclodextrin-modified urease to create nanovalves to seal holes in the MSNPs (Fig. 4C) [56]. Because of the blocking effect of the nanovalve, drug release was hindered at physiological pH levels; however, protonation of the benzimidazole group enabled the release control of the supramolecular nanovalve-bound drug, specifically under acidic lysosomal conditions. This advancement has facilitated the development of gated enzyme-driven motors capable of on-demand payload delivery based on predetermined environmental stimuli such as acidity or alkalinity, thereby preventing drug leakage.

Despite significant advancements in laboratory settings, the translation of UMNMs into clinical applications has been impeded by limited investigations of collective motor behavior and *in vivo* tracking imaging. To address this issue, Sánchez and co-workers [2] radiolabeled mesoporous silica nanomodels with either ^{124}I on gold

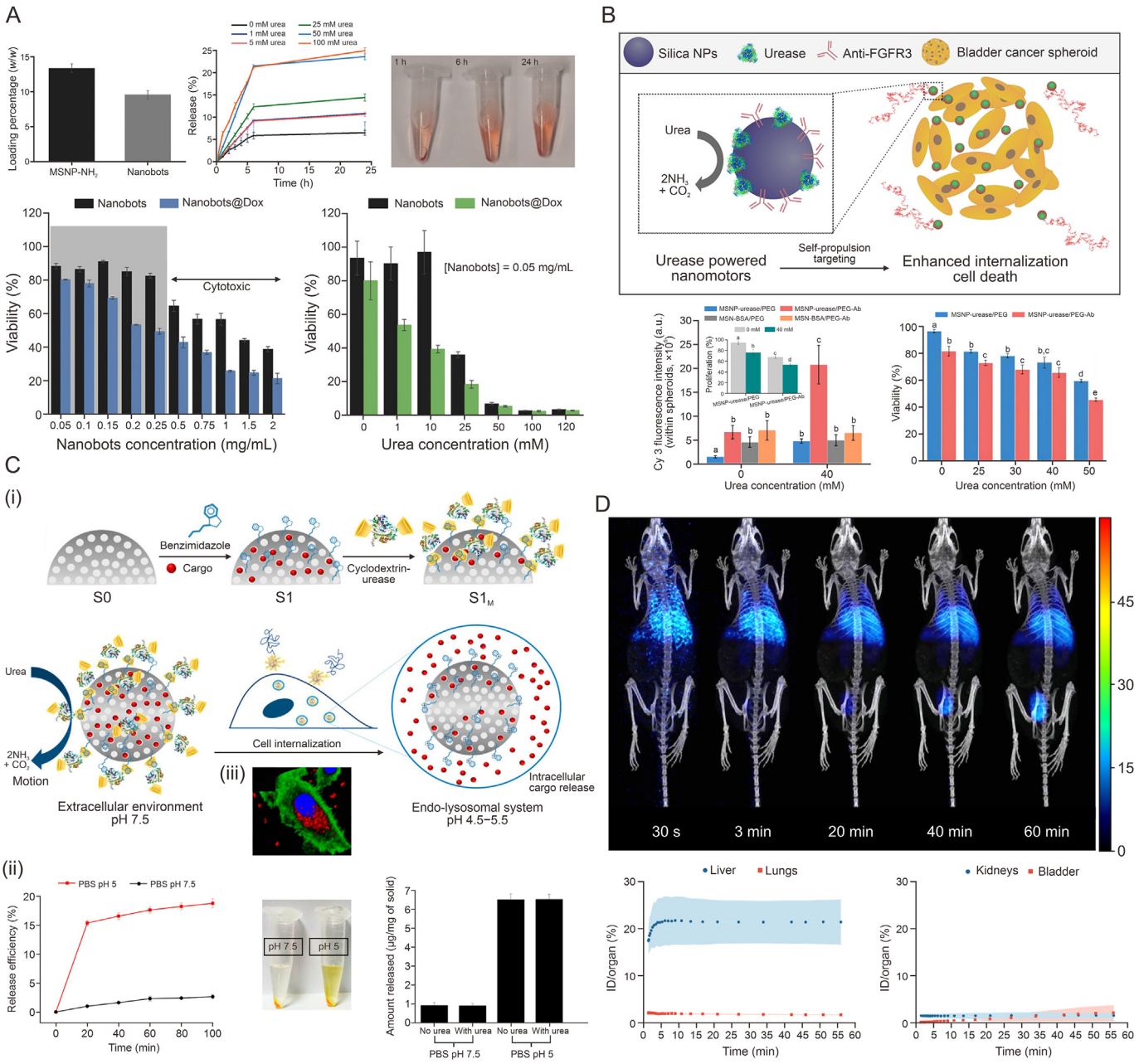

Fig. 4. Urease-powered micro/nanomotors (MNMs) (UMNMs) for treating bladder tumor. (A) Evaluation of UMNMs as drug carriers [52]. (B) UMNMs for active targeting of bladder cancer spheroids [53]. Different superscripts denote significant differences among groups with $P < 0.05$. (C) Enzyme-powered stimuli-responsive nanomotors for on-command intracellular payload delivery [56]. (D) Analysis of the biodistribution of ^{18}F-labeled UMNMs injected intravenously in female mice [2]. MSNP: mesoporous silica nanoparticle (NP); FGFR3: fibroblast growth factor receptor 3; PEG: polyethylene glycol; BSA: bovine serum albumin; Ab: antibody. Reprinted from Refs. [2,52,53,56] with permission.

NPs or ^{18}F-labeled prosthetic group to urease. They extensively examined the swarming behavior of these models and tracked their performance by PET technology (Fig. 4D). These findings showed the ability to track positron emitter-labeled nanomotors in living organisms using PET imaging after administration, and indicate their high radiochemical stability *in vivo*. This study established a foundation for the utilization of enzyme nanomotors in biomedical applications and represents, a significant advancement in clinical treatments.

5.2. Biological barrier

Antineoplastic drugs must overcome various physiological barriers before reaching the target tumor cells. Addressing these transport obstacles is an effective strategy for enhancing motor motility and optimizing drug delivery efficiency. For instance, Zhang et al. [122] developed DOX-loaded Janus micromotors inspired by an icebreaker design, incorporating urease for propulsion and hyaluronidase to degrade the dense extracellular matrix (ECM) within tumor tissues (Fig. 5A). ECM digestion in the diffusion pathway enhanced drug retention and diffusion within the tumor more effectively than enzyme-mediated movement. The ECM digestion and motility capabilities of Janus nanomotors do not affect the endocytic mechanism but result in a cellular uptake that is over 3-fold higher than that of the original Janus nanorods.

Similarly, Sánchez and co-workers [123] devised two different swarms of nanomotors that leveraged their active movement and swarm behavior to overcome biological barriers and enhance drug

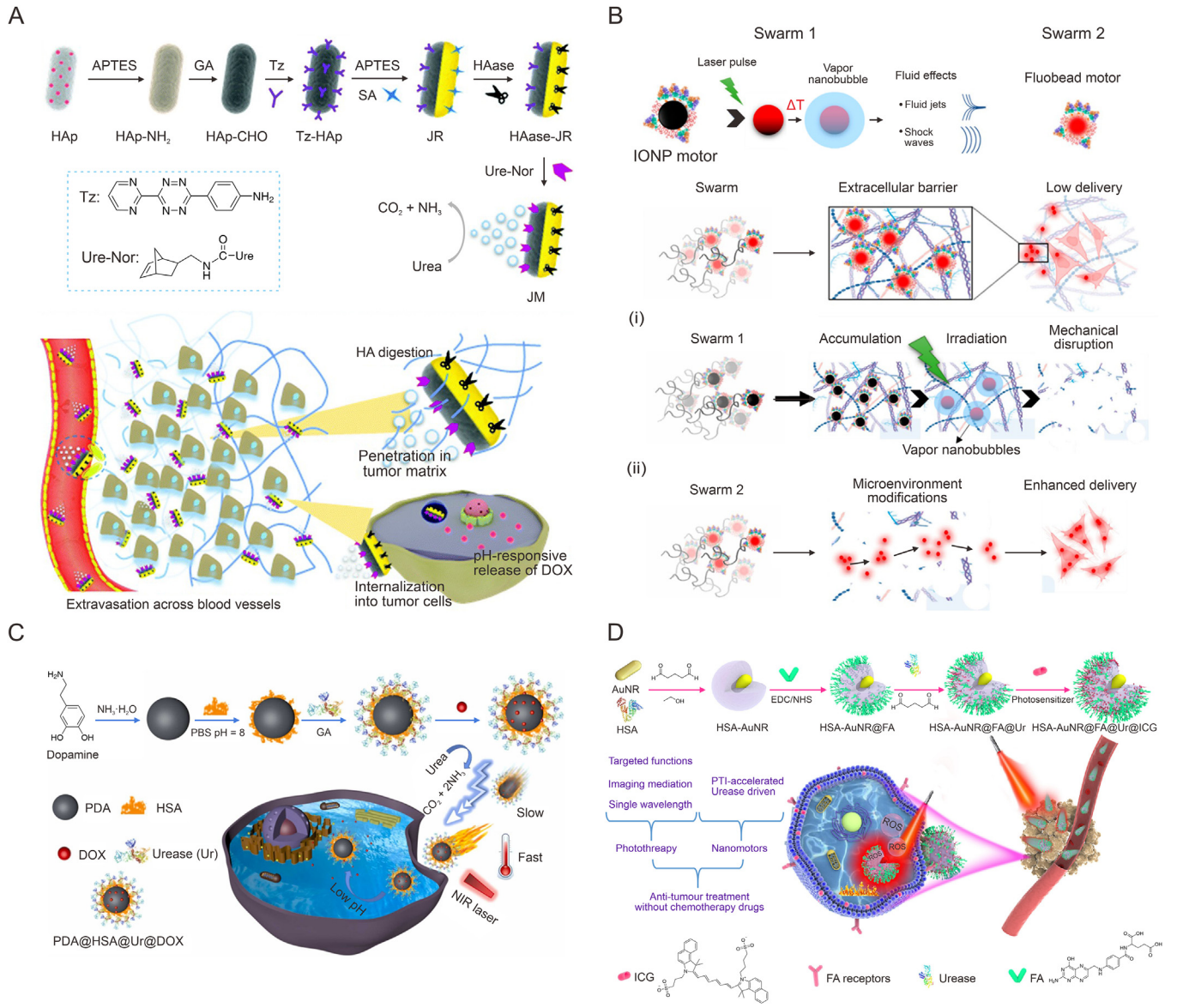

Fig. 5. Urease-powered micro/nanomotors (MNMs) (UMNMs) for overcoming the delivery barriers and optical therapy. (A) Icebreaker-inspired UMNMs to overcome the delivery barriers and enhance cellular internalization and cytotoxicity [122]. (B) Swarms of UMNMs for enhanced delivery efficiency [123]. (C) Urease-powered polydopamine (PDA) nanomotors with enhanced anticancer efficacy [61]. (D) Urease-powered human serum albumin (HSA) nanomotor for photothermal and photodynamic cancer combination therapy [83]. HAp: hydroxyapatite; APTES: 3-aminopropyltriethoxysilane; GA: glutaraldehyde; Tz: tetrazine; SA: succinic anhydride; JR: Janus nanorod; HAase: hyaluronidase; Ure-Nor: norbornene-terminated urease; JM: Janus nanomotor; HA: hyaluronic acid; IONPs: iron oxide nanoparticles (NPs); DOX: doxorubicin; FA: folic acid; EDC: 1-ethyl-3 (3-dimethylaminopropyl) carbodiimide; NHS: *N*-hydroxysuccinimide; ICG: indocyanine green. Reprinted from Refs. [61,83,122,123] with permission.

transport (Fig. 5B). Specifically, swarm 1 consists of iron oxide NPs propelled by urease, which aggregate on type I collagen fibers. Laser irradiation triggered the formation of vapor nanobubbles (VNB) that can disrupt the biological barrier model and reduce steric hindrance. The efficiency of drug transport was evaluated based on the ability of swarm 2, composed of urease-driven PS beads, to traverse the disrupted barrier and be internalized by HeLa cells located on the opposite sides. The experiments exhibited an obvious improvement in delivery efficiency following the disrupted biological barrier, with a 10-fold increase observed in the group subjected to 10 laser pulses. The synergistic interplay between the active movement and mechanical disruption of biological barriers has immense potential for augmenting current therapeutic approaches hindered by inadequate drug delivery vehicles crossing these barriers.

5.3. Optical therapy

Although researchers have made significant advancements in enhancing drug delivery efficiency and achieving precise controlled drug release, there are still challenges associated with radiotherapy drugs such as their high toxicity and limited scope of application. As an emerging modality for disease treatment, organic or inorganic material-based optical therapy exhibits noninvasiveness, minimal adverse reactions, and notable targeting capabilities [124]. PTT uses photosensitive materials to generate enough heat under NIR irradiation to induce thermal damage or ablate cells [125]. Photodynamic therapy (PDT) take advantages of the photosensitizer to absorb laser energy at a specific wavelength and subsequently deliver it to surrounding oxygen molecules, thereby generating ROS that inflict damage to the cell membrane and induce cellular death [126]. Optical

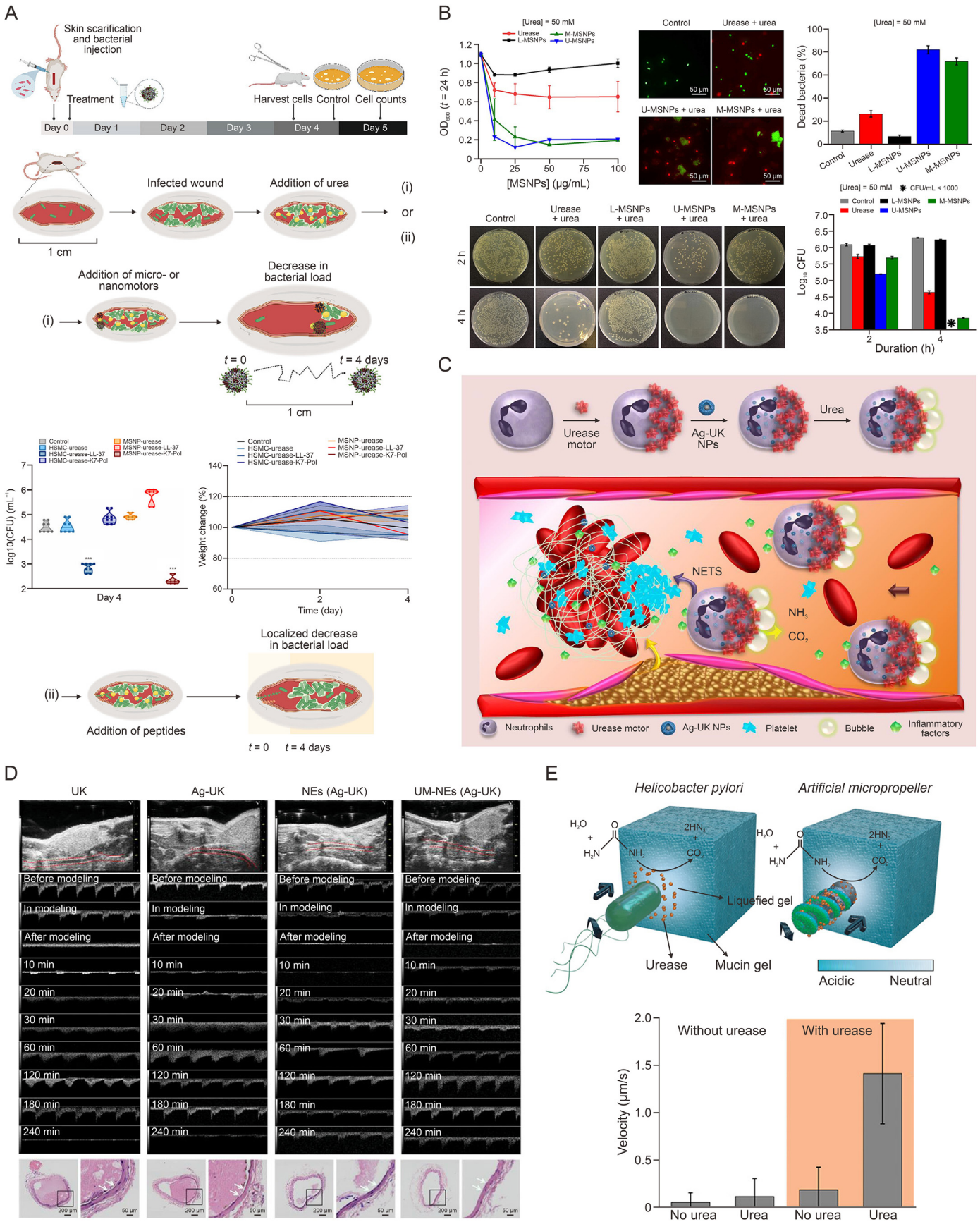

Fig. 6. Urease-powered micro/nanomotors (MNMs) (UMNMs) for antibacterial, antithrombotic, and stomach disease treatment. (A) UMNMs for antimicrobial treatment [54]. (B) Evaluating the bactericidal capacity of the different enzyme-based micromotors [128]. (C) UMNMs used as drug delivery systems for thrombolytic therapy [78]. (D) *In vivo*

therapy can be employed either independently or in conjunction with drug therapy to yield potent antitumor effects. Mussel-inspired PDA has been extensively investigated owing to its significant photothermal conversion efficiency and effective NIR-to-thermal energy conversion capability. Shuai and co-workers [61] developed a urease-driven PDA nanomotor that exhibited temperature elevation in the tumor microenvironment with NIR laser irradiation (Fig. 5C). This temperature increase not only induced the apoptosis of tumor cells but also improved the catalytic activity of urease, thereby promoting the movement of the nanomotor and facilitating cell internalization. In addition, the nanomotors exhibited enhanced anticancer efficacy, which was attributed to the synergistic interplay between photothermal and chemotherapy modalities. This study introduces a novel approach: photothermal interventions (PTIs) with UMNMs, which enables efficient heat-assisted cancer treatment within complex physiological environments by leveraging improved motility and synergistic therapeutic effects.

Subsequently, they developed a urease-driven HSA nanomotor loaded with folic acid (FA) and ICG, aiming to achieve drug-free phototherapy (Fig. 5D) [83]. ICG exhibited excellent photothermal conversion ability, enabling a localized temperature increase under NIR irradiation. This not only achieved cell-killing effects but also enhanced urease activity within a specific temperature range, thereby improving motor movement capability. The experiments showed that the motor gradually generated ROS during laser irradiation, thereby enhancing the efficacy of drug-free phototherapy. Moreover, the photosensitizer ICG allows the real-time monitoring of the cellular uptake efficiency of the nanomotor during treatment.

The PTI nanomotor enhanced movement ability, thereby improving the cellular uptake and exhibiting a favorable phototherapeutic effect, thus offering the potential for chemotherapy-free tumor treatment. However, achieving *in situ* treatment of tumors in other body parts remains a challenge, necessitating further exploration of motors for targeted therapy.

5.4. Antimicrobial treatment

Bacterial infections represent a major risk to human health. Owing to the overuse of antibiotics, drug-resistant bacteria have emerged and spread widely, posing a major threat to public health [127]. The utilization of MNMs as carriers for delivering antibacterial agents can greatly enhance their therapeutic efficacy. Their exceptional mobility not only helps the diffusion and retention of pharmaceuticals at the infection site, but also promotes their interaction with bacteria, offering a novel strategy for the efficient delivery of antibacterial agents. Arqué et al. [54] have conducted experiments that loaded antimicrobial peptides (AMP) onto the surface of urease-driven silica MNMs (Fig. 6A). The results showed that in a the mouse model infected with *Acinetobacter baumannii* on its back, AMP-modified MNMs exhibited significant autonomous propulsion ability, resulting in a 2−3 orders of magnitude reduction in the bacterial load at the infected wound site, while exerting an antibacterial effect far from the administration site.

To mitigate the adverse effects of antimicrobial drugs and the emergence of drug-resistant bacteria, Sánchez and co-workers [128] developed enzyme-based nanomotors devoid of bactericidal drugs targeting bacteria modified with urease (U-MSNPs), lysozyme (L-MSNPs), or both urease and lysozyme (M-MSNPs), and evaluated their efficacy against pathogenic *Escherichia coli* (*E. coli*) (Fig. 6B). These findings revealed that lysozyme had a negligible impact on Gram-negative *E. coli* and did not exhibit bactericidal activity. However, owing to the presence of bicarbonate and NH_3, both U-MSNPs and M-MSNPs exhibited bactericidal properties as byproducts of urea hydrolysis. Notably, U-MSNPs exhibited superior effectiveness in reducing 60% of the biomass biofilm of uropathogenic *E. coli* at a concentration of 200 μg/mL.

Photothermal antibacterial therapy is an innovative therapeutic approach that converts NIR light energy into heat using photothermal agents, thereby increasing local temperatures to treat bacterial infections with thermal ablation [129]. Ma and co-workers [109] successfully loaded urease and antibacterial drugs onto PDA-coated liquid-metal NPs, enabling synergistic antibacterial effects by combining PTT and chemotherapy. Upon NIR light irradiation, the nanomotors underwent morphological changes, presenting a promising strategy for overcoming medical and biological barriers. The viability of *E. coli* cells treated with the LMs decreased significantly to 57.1% after light irradiation, indicating the feasibility of PTT.

5.5. Antithrombotic therapy

Thrombosis occurs because of platelet recruitment to the site of vascular endothelial damage, and the intricate interplay between platelets and various plasma proteins culminates in the formation of insoluble plaques that impede normal blood flow [130]. Thrombosis is a pivotal event in the development of mortal cardiovascular conditions like myocardial infarction and ischemic stroke [131]. Challenges associated with thrombosis treatment include a limited drug half-life, suboptimal utilization rates, and inadequate thrombus site permeability. Current therapeutic approaches struggle to attain desired efficacy levels.

NEs can actively target the thrombus site and release NETs after activated by inflammatory cytokines. Although these inherent characteristics make NEs excellent carriers for thrombolytic drugs, there is a lack of sufficient driving force to overcome the blood flow resistance. Therefore, Sang and co-workers [78] devised a NEs delivery system powered by urease to transport the thrombolytic drug Ag-UK, enabling active targeting of the thrombus site and facilitating effective treatment of thrombosis (Fig. 6C). The results showed that the intravenous UM-NEs (Ag-UK) system exhibited rapid targeting of the thrombus site, activation by inflammatory factors enriched in blood vessels, and subsequent release of NETs to facilitate the liberation of Ag-UK. Ag-UK can induce thrombolysis and vascular recanalization (Fig. 6D) [78]. This system is expected to be used in the clinical treatment of thrombotic diseases.

5.6. Gastric diseases

Oral administration offers significant advantages for treating gastrointestinal disorders and is the most common drug delivery route [132]. However, gastrointestinal physiological barriers like gastric acid secretion, mucus layer formation, and epithelial barrier integrity pose substantial challenges to effective drug delivery. Therefore, to increase the efficacy of oral drug administration, efficient delivery systems that can overcome these obstacles are essential. The unique capabilities of active propulsion and deep tissue penetration endow MNMs with significant potential for application in oral drug delivery systems (ODDS), an area extensively explored by researchers, including chemical propulsion, external field propulsion, and biological propulsion. Each type of MNMs exhibits distinct characteristics in effectively penetrated the physiological barrier in the gastrointestinal tract. *Helicobacter pylori* (*H. pylori*) can secrete urease, neutralize the local pH and induce a

thrombolysis effect evaluation [78]. (E) The surface-immobilized urease-powered biomimetic micropropellers to overcome the mucus barrier [134]. MSNPs: mesoporous silica nanoparticles (NPs); HSMPs: hollow silica microparticles; U-MSNPs: urease-MSNPs; L-MSNPs: lysozyme-MSNPs; M-MSNPs: urease and lysozyme-MSNPs; NEs: neutrophils; NETs: NE extracellular traps; Ag-UK NPs: urokinase (UK) coupled silver (Ag) NPs; UM-NEs: urease micromotor powered Janus NEs. Reprinted from Refs. [54,78,128,134] with permission.

gel-sol transition of the mucus layer. Inspired by this, researchers have directed their attention toward using UMNMs to explore novel approaches for enhancing motor permeability [133]. Walker et al. [134] mimicked the strategy of *H. pylori* to overcome the mucus barrier by incorporating urease onto the surface of magnetic micropropellers to disrupt the mucus layer and facilitate motor movement (Fig. 6E). The experimental findings showed that these motors with urea substrate efficiently penetrated the mucus barrier.

PDA, a highly adhesive material, exhibits a prolonged retention time within the organisms. Choi et al. [62] successfully developed UMNMs based on PDA. *In vivo* tests showed enhanced permeability and extended gastric retention of these micromotors for 24 h, followed by complete clearance within 3 days without inducing any gastrointestinal toxicity.

Given the detrimental impact of the highly acidic gastric environment on urease activity, extensive efforts have been dedicated to safeguarding its enzymatic function. Sánchez and co-workers [67] successfully devised two distinct types of liposomal nanomotors propelled by urease, wherein one was encapsulated within the liposome and the other was electrostatically attached to its outer surface. Asymmetric distribution is induced by random electrostatic binding of urease to liposome outer surface and drives the movement of MNM motors. However, when exposed to harsh environments such as extremely low pH in the stomach, its activity and motility are compromised. Urease encapsulated within the lipid bilayer provides protection against acidic conditions such as those found in the stomach. Moreover, by regulating the fluidity of the lipid bilayer using sodium deoxycholate (naturally present in the gastrointestinal tract), we can significantly enhance the mobility of nanomotors encapsulated with urease. After a 1-h incubation under these conditions, the liposomal nanomotors were able to resume their movement. This study presents new possibilities for efficient delivery of drugs to the gastrointestinal tract.

6. Challenges and future prospects

Researchers have paid considerable attention to the biosafety and biocompatibility of enzyme-driven MNMs, resulting in remarkable advancements in this field. This review outlines the framework materials used for the fabrication of UMNMs, their motion regulation, and their progress in disease detection, diagnosis, and treatment. Despite injecting new vitality into biomedical development, the utilization of UMNMs in clinical settings faces numerous limitations and challenges [119] (Fig. 7).

6.1. How to survive in vivo environment

The preservation of urease activity is crucial for maintaining the stability and self-propulsion of nanomotors in complex *in vivo* environments. Ensuring that enzymatic catalytic activity remains intact, while minimizing immune system recognition is essential for the successful application of EMNMs *in vivo*. Currently, most studies investigating the motor behavior of UMNMs use solutions with simple components that fail to accurately represent complex environments such as blood. In these environments, various proteins present in plasma form a “protein corona” on the motor surface, obstructing catalytic reactions and attenuating motor behavior to some extent [135].

To maintain motor mobility, it is imperative to explore the design of motors driven by a combination of modalities, such as light, ultrasound, or magnetic fields [5,6,9–12]. According to a study, less than 1% of NPs in targeted cancer therapies can overcome various physical and biological barriers to reach tumor tissue [136], and this conclusion may also apply to MNMs. Enhancing the survival of living organisms necessitates the fabrication of motors using materials that exhibit excellent biocompatibility. Recently, there has been growing interest in cell membrane-coated NPs as a research focus area, offering a novel approach to shield MNMs from immune system clearance [72].

6.2. How to locate and reach targets

To achieve precise motor control to target diseased sites, MNMs must locate and accurately reach the specified site after addressing the issue of survival within the body. Although UMNMs exhibit chemotaxis toward areas with high urea concentrations, which is beneficial for treating urinary system diseases, particularly bladder diseases, they may not guarantee sufficient precision in the targeted movement. A viable solution involves the attachment of binding antibodies, which can specifically bind to the lesion site, to the external surface of the motor. Sánchez and co-workers [53] successfully linked an anti-FGFR3 antibody to the surface of UMNMs for to target bladder cancer cells, illustrating their potential as a targeted therapy tool.

However, during self-propulsion, the motor encounters various biological barriers, such as the ECM in tumors and the mucosal layer of the gastric wall, which restrict its penetration into the diseased tissue. Therefore, researchers are considering MNMs that can effectively overcome these biological barriers *in vivo*. Inspired by *H. pylori*, they developed urease-driven PDA micromotors [62]. Urease hydrolysis of urea releases NH_3, raising local pH and inducing gel-sol transition in the gastric mucosa. This enabled easier penetration of the motor through the gastric wall and prolonged its

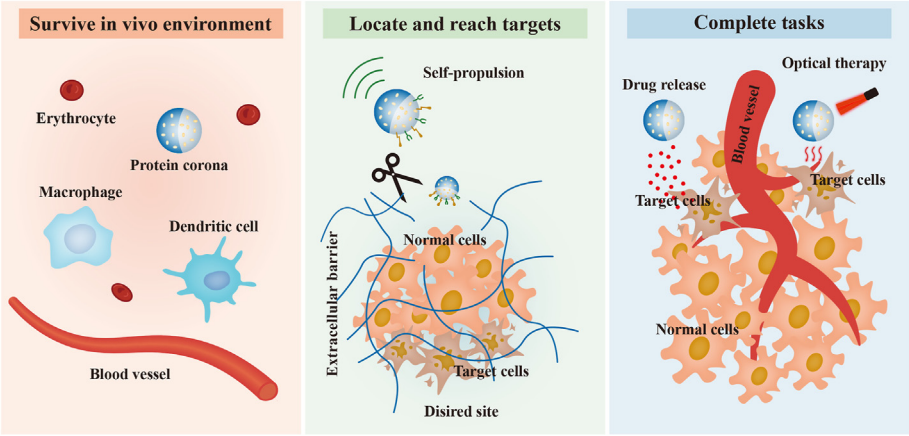

Fig. 7. Challenges in the clinical application of urease-powered micro/nanomotors (MNMs) (UMNMs).

residence time. Furthermore, it is possible to design two types of motors to work together: one for breaking down biological barriers and the other for penetrating the target tissue for treatment [123].

We relied on medical imaging technology to verify the precise localization of nanomotors within the body. Various techniques, including radionuclide, fluorescence, and ultrasound imaging, have been used to visualize and track nanomotor movement *in vivo* [2,83,109]. Although these technologies are still in the nascent stages and achieving true real-time 3D tracking remains a formidable challenge, we remain optimistic regarding the advancement and clinical implementation of nanomotor imaging technology. The current obstacles will not impede its progress or translational potential.

6.3. How to complete tasks precisely

The primary criterion for evaluating nanomotors, regardless of their speed, targeting ability, and biocompatibility, is their ability to accurately diagnose and treat diseases. Currently, the most extensively researched application of motors in biomedicine is drug delivery. Scientists have focused on achieving precise drug release at the intended target location. It has been possible to regulate the release of medications inserted into MSNP pores by using pH-responsive polymers [56]. Alternatively, a motor can be fabricated using substances exhibiting stimulus-response characteristics and loaded with drugs, thereby enabling drug release upon exposure to the corresponding stimulus. NEs active targeting capabilities toward inflammatory sites and subsequently release NETs following activation by inflammatory cytokines. Sang and co-workers [78] used this feature to design a urease-driven NEs delivery system for carrying the thrombolytic drug Ag-UK.

In addition to chemotherapy, MNMs can be used in alternative therapies, including PTT [125] and PDT [126]. PDA has garnered significant attention because of its excellent biocompatibility and high photothermal conversion efficiency [46,61,62]. MNMs fabricated using PDA NPs or coated with a layer of PDA film on their surface can induce cell death when exposed to NIR light, resulting in a localized temperature elevation. Simultaneous enhancement of the catalytic activity of urease can facilitate penetration of the motor into the affected site, thereby augmenting its therapeutic efficacy. Combining chemotherapy with phototherapy not only improves treatment precision and effectiveness but also reduces reliance on chemotherapeutic drugs, thus mitigating their associated side effects to a certain extent. Achieving precise disease treatment, enhancing efficacy, and minimizing adverse reactions have always posed challenges in the clinical translation of MNMs, while simultaneously reflecting their application value. In summary, despite the promising advancements in the field of biomedical UMNMs, a substantial gap remains between *in vitro* studies and clinical applications. Drawing upon the current research progress, this paper provides an overview of the potential problems UMNMs face as they continue to evolve, while proposing viable solutions. It is anticipated that through extensive research efforts, the advancement and implementation of MNMs will yield groundbreaking breakthroughs in the realm of biomedicine.

7. Conclusion

UMNMs exhibit excellent biocompatibility, self-propulsion capabilities for targeted disease localization, and robust payload capacities, thereby promoting advancements in disease diagnosis, medical imaging, and novel drug delivery systems. This indicates broad prospects for application and offers novel opportunities for intelligent diagnosis and precise treatment in the biomedical field. Recent studies have revealed the immense potential of UMNMs for imaging, biological detection, and targeted drug delivery. In addition, the integration of multiple imaging techniques and therapeutic methods with the high loading capacity and mobility of nanomotors enables diagnosis and treatment on a single platform, facilitating image-guided therapy and opening novel avenues for clinical applications. In conclusion, although some achievements have been made, there remains a considerable journey from *in vitro* investigations to practical *in vivo* applications. First, nanomotors have significant advantages owing to their autonomous propulsion; however, whether this movement can be guaranteed in the human physiological environment remains unclear. In addition, the active movement of the motor may cause mechanical damage to the surrounding tissues and cells. Second, although researchers have designed smart motors for different applications, such as using temperature-sensitive and pH-sensitive materials, to respond to surrounding environmental changes, it is still a big challenge to respond appropriately to an internal environment with multiple variables, as opposed to responding to a specific external stimulus. Therefore, we make the following recommendations for further development of EMNMs. First, as the power source for the motor, the enzyme must be firmly linked to a specific area of the micro/nanomotor, while maintaining the necessary activity of the enzyme. To improve the safety and therapeutic effects, it is necessary to reasonably predict the movement trajectory and accurately control the movement direction and speed of EMNMs to achieve accurate positioning of the desired location and targeted therapy. In addition, the biomedical application of nanomotors requiries multidisciplinary knowledge, including biology, chemistry, materials, and physics. It is expected that more theoretical knowledge and collaboration between different disciplines will bring inspiring ideas and make breakthroughs in the development of EMNMs. We anticipate that this review will highlight the recent advancements of UMNMs in the biomedical field and ultimately advance their successful exploration in clinical settings.

CRediT authorship contribution statement

Wen-Wen Li: Writing – original draft, Data curation. **Zi-Li Yu:** Writing – review & editing, Funding acquisition. **Jun Jia:** Writing – review & editing.

Declaration of competing interest

The authors declare that there are no conflicts of interest.

Acknowledgments

This work was supported by the National Natural Science Foundation of China (Grant No.: 82372102).

References

[1] R.D. Vale, R.A. Milligan, The way things move: Looking under the hood of molecular motor proteins, Science 288 (2000) 88–95.
[2] A.C. Hortelao, C. Simó, M. Guix, et al., Swarming behavior and *in vivo* monitoring of enzymatic nanomotors within the bladder, Sci. Robot. 6 (2021), eabd2823.
[3] T. Patiño, N. Feiner-Gracia, X. Arqué, et al., Influence of enzyme quantity and distribution on the self-propulsion of non-Janus urease-powered micromotors, J. Am. Chem. Soc. 140 (2018) 7896–7903.
[4] X. Ma, A. Jannasch, U.-R. Albrecht, et al., Enzyme-powered hollow mesoporous Janus nanomotors, Nano Lett. 15 (2015) 7043–7050.
[5] L. Xu, F. Mou, H. Gong, et al., Light-driven micro/nanomotors: From fundamentals to applications, Chem. Soc. Rev. 46 (2017) 6905–6926.
[6] X. Zeng, M. Yang, H. Liu, et al., Light-driven micro/nanomotors in biomedical applications, Nanoscale 15 (2023) 18550–18570.
[7] P. Calvo-Marzal, S. Sattayasamitsathit, S. Balasubramanian, et al., Propulsion

of nanowire diodes, Chem. Commun. (Camb) 46 (2010) 1623–1624.
[8] S.T. Chang, E. Beaumont, D.N. Petsev, et al., Remotely powered distributed microfluidic pumps and mixers based on miniature diodes, Lab Chip 8 (2008) 117–124.
[9] S. Tottori, L. Zhang, F. Qiu, et al., Magnetic helical micromachines: Fabrication, controlled swimming, and cargo transport, Adv. Mater. 24 (2012) 811–816.
[10] A. Ghosh, P. Fischer, Controlled propulsion of artificial magnetic nanostructured propellers, Nano Lett. 9 (2009) 2243–2245.
[11] M. Uygun, B. Jurado-Sánchez, D.A. Uygun, et al., Ultrasound-propelled nanowire motors enhance asparaginase enzymatic activity against cancer cells, Nanoscale 9 (2017) 18423–18429.
[12] T. Xu, L.-P. Xu, X. Zhang, Ultrasound propulsion of micro-/nanomotors, Appl. Mater. Today 9 (2017) 493–503.
[13] H. Zhao, Y. Zheng, Y. Cai, et al., Intelligent metallic micro/nanomotors: From propulsion to application, Nano Today 52 (2023), 101939.
[14] S. Palagi, P. Fischer, Bioinspired microrobots, Nat. Rev. Mater. 3 (2018) 113–124.
[15] J. Li, B. Esteban-Fernández de Ávila, W. Gao, et al., Micro/nanorobots for biomedicine: Delivery, surgery, sensing, and detoxification, Sci. Robot. 2 (2017), eaam6431.
[16] F. Soto, J. Wang, R. Ahmed, et al., Medical micro/nanorobots in precision medicine, Adv. Sci. (Weinh) 7 (2020), 2002203.
[17] J. Ou, K. Liu, J. Jiang, et al., Micro-/nanomotors toward biomedical applications: The recent progress in biocompatibility, Small 16 (2020), 1906184.
[18] M. Mathesh, J. Sun, D.A. Wilson, Enzyme catalysis powered micro/nanomotors for biomedical applications, J. Mater. Chem. B 8 (2020) 7319–7334.
[19] H. Fang, J. Chen, L. Lin, et al., A strategy of killing three birds with one stone for cancer therapy through regulating the tumor microenvironment by H_2O_2-responsive gene delivery system, ACS Appl. Mater. Interfaces 11 (2019) 47785–47797.
[20] S. Keller, S.P. Teora, G.X. Hu, et al., High-throughput design of biocompatible enzyme-based hydrogel microparticles with autonomous movement, Angew. Chem. Int. Ed Engl. 57 (2018) 9814–9817.
[21] B.V.V.S. Pavan Kumar, A.J. Patil, S. Mann, Enzyme-powered motility in buoyant organoclay/DNA protocells, Nat. Chem. 10 (2018) 1154–1163.
[22] S. Parvez, M.J.C. Long, J.R. Poganik, et al., Redox signaling by reactive electrophiles and oxidants, Chem. Rev. 118 (2018) 8798–8888.
[23] H.J. Forman, A. Bernardo, K.J. Davies, What is the concentration of hydrogen peroxide in blood and plasma? Arch. Biochem. Biophys. 603 (2016) 48–53.
[24] B. Halliwell, M.V. Clement, L.H. Long, Hydrogen peroxide in the human body, FEBS Lett. 486 (2000) 10–13.
[25] G. Pizzino, N. Irrera, M. Cucinotta, et al., Oxidative stress: Harms and benefits for human health, Oxid. Med. Cell. Longev. 2017 (2017), 8416763.
[26] H. Li, Z. Sun, S. Jiang, et al., Tadpole-like unimolecular nanomotor with sub-100 nm size swims in a tumor microenvironment model, Nano Lett. 19 (2019) 8749–8757.
[27] B.J. Toebes, L.K.E.A. Abdelmohsen, D.A. Wilson, Enzyme-driven biodegradable nanomotor based on tubular-shaped polymeric vesicles, Polym. Chem. 9 (2018) 3190–3194.
[28] Y. Xie, S. Fu, J. Wu, et al., Motor-based microprobe powered by bio-assembled catalase for motion detection of DNA, Biosens. Bioelectron. 87 (2017) 31–37.
[29] L. Liu, H. Mo, S. Wei, et al., Quantitative analysis of urea in human urine and serum by 1H nuclear magnetic resonance, Analyst 137 (2012) 595–600.
[30] L. Schwarz, M. Medina-Sánchez, O.G. Schmidt, Hybrid BioMicromotors, Appl. Phys. Rev. 4 (2017), 031301.
[31] S. Anu Mary Ealia, M.P. Saravanakumar, A review on the classification, characterisation, synthesis of nanoparticles and their application, IOP Conf. Ser. Mater. Sci. Eng. 263 (2017), 032019.
[32] V.J. Mohanraj, Y. Chen, Nanoparticles - A review, Trop. J. Pharm. Res. 5 (2007) 561–573.
[33] L.-F. Chen, C.-C. Hou, L. Zou, et al., Uniformly bimetal-decorated holey carbon nanorods derived from metal-organic framework for efficient hydrogen evolution, Sci. Bull. (Beijing) 66 (2021) 170–178.
[34] Y. Bai, G. Zhang, S. Zheng, et al., Pyridine-modulated Ni/Co bimetallic metal-organic framework nanoplates for electrocatalytic oxygen evolution, Sci. China Mater. 64 (2021) 137–148.
[35] X. Yao, D. Chen, B. Zhao, et al., Acid-degradable hydrogen-generating metal-organic framework for overcoming cancer resistance/metastasis and off-target side effects, Adv. Sci. (Weinh) 9 (2022), e2101965.
[36] S. Mallakpour, E. Nikkhoo, C.M. Hussain, Application of MOF materials as drug delivery systems for cancer therapy and dermal treatment, Coord. Chem. Rev. 451 (2022), 214262.
[37] S. Huang, X. Kou, J. Shen, et al., "Armor-plating" enzymes with metal–organic frameworks (MOFs), Angew. Chem. Int. Ed. Engl. 59 (2020) 8786–8798.
[38] S. Yuan, L. Feng, K. Wang, et al., Stable metal-organic frameworks: Design, synthesis, and applications, Adv. Mater. 30 (2018), e1704303.
[39] K.S. Park, Z. Ni, A.P. Côté, et al., Exceptional chemical and thermal stability of zeolitic imidazolate frameworks, Proc. Natl. Acad. Sci. USA 103 (2006) 10186–10191.
[40] H. Yang, L. Wang, X. Huang, MOF-based micro/nanomotors (MOFtors): Recent progress and challenges, Coord. Chem. Rev. 495 (2023), 215372.
[41] A. Terzopoulou, X. Wang, X. Chen, et al., Biodegradable metal-organic framework-based microrobots (MOFBOTs), Adv. Healthc. Mater. 9 (2020), e2001031.
[42] X. Wang, X. Chen, C.C.J. Alcântara, et al., MOFBOTS: Metal-organic-framework-based biomedical microrobots, Adv. Mater. 31 (2019), 1901592.
[43] B. Wu, J. Fu, Y. Zhou, et al., Tailored core shell dual metal-organic frameworks as a versatile nanomotor for effective synergistic antitumor therapy, Acta Pharm. Sin. B 10 (2020) 2198–2211.
[44] Y. You, D. Xu, X. Pan, et al., Self-propelled enzymatic nanomotors for enhancing synergetic photodynamic and starvation therapy by self-accelerated cascade reactions, Appl. Mater. Today 16 (2019) 508–517.
[45] K. Liang, R. Ricco, C.M. Doherty, et al., Biomimetic mineralization of metal-organic frameworks as protective coatings for biomacromolecules, Nat. Commun. 6 (2015), 7240.
[46] B.K. Kaang, L. Ha, J.-U. Joo, et al., Laminar flow-assisted synthesis of amorphous ZIF-8-based nano-motor with enhanced transmigration for photothermal cancer therapy, Nanoscale 14 (2022) 10835–10843.
[47] S.-H. Wu, C.-Y. Mou, H.-P. Lin, Synthesis of mesoporous silica nanoparticles, Chem. Soc. Rev. 42 (2013) 3862–3875.
[48] C. Argyo, V. Weiss, C. Bräuchle, et al., Multifunctional mesoporous silica nanoparticles as a universal platform for drug delivery, Chem. Mater. 26 (2014) 435–451.
[49] Z. Chen, T. Xia, Z. Zhang, et al., Enzyme-powered Janus nanomotors launched from intratumoral depots to address drug delivery barriers, Chem. Eng. J. 375 (2019), 122109.
[50] X. Arqué, A. Romero-Rivera, F. Feixas, et al., Intrinsic enzymatic properties modulate the self-propulsion of micromotors, Nat. Commun. 10 (2019), 2826.
[51] T. Patino, A. Porchetta, A. Jannasch, et al., Self-sensing enzyme-powered micromotors equipped with pH-responsive DNA nanoswitches, Nano Lett. 19 (2019) 3440–3447.
[52] A.C. Hortelão, T. Patiño, A. Perez-Jiménez, et al., Enzyme-powered nanobots enhance anticancer drug delivery, Adv. Funct. Mater. 28 (2018), 1705086.
[53] A.C. Hortelão, R. Carrascosa, N. Murillo-Cremaes, et al., Targeting 3D bladder cancer spheroids with urease-powered nanomotors, ACS Nano 13 (2019) 429–439.
[54] X. Arqué, M.D.T. Torres, T. Patiño, et al., Autonomous treatment of bacterial infections *in vivo* using antimicrobial micro- and nanomotors, ACS Nano 16 (2022) 7547–7558.
[55] X. Ma, X. Wang, K. Hahn, et al., Motion control of urea-powered biocompatible hollow microcapsules, ACS Nano 10 (2016) 3597–3605.
[56] A. Llopis-Lorente, A. García-Fernández, N. Murillo-Cremaes, et al., Enzyme-powered gated mesoporous silica nanomotors for on-command intracellular payload delivery, ACS Nano 13 (2019) 12171–12183.
[57] R.K. Kankala, Y.-H. Han, J. Na, et al., Nanoarchitectured structure and surface biofunctionality of mesoporous silica nanoparticles, Adv. Mater. 32 (2020), e1907035.
[58] T. Priemel, G. Palia, F. Förste, et al., Microfluidic-like fabrication of metal ion-cured bioadhesives by mussels, Science 374 (2021) 206–211.
[59] Y. Liu, K. Ai, L. Lu, Polydopamine and its derivative materials: Synthesis and promising applications in energy, environmental, and biomedical fields, Chem. Rev. 114 (2014) 5057–5115.
[60] H. Li, D. Yin, W. Li, et al., Polydopamine-based nanomaterials and their potentials in advanced drug delivery and therapy, Colloids Surf. B Biointerfaces 199 (2021), 111502.
[61] M. Wu, S. Liu, Z. Liu, et al., Photothermal interference urease-powered polydopamine nanomotor for enhanced propulsion and synergistic therapy, Colloids Surf. B Biointerfaces 212 (2022), 112353.
[62] H. Choi, S.H. Jeong, T.Y. Kim, et al., Bioinspired urease-powered micromotor as an active oral drug delivery carrier in stomach, Bioact. Mater. 9 (2021) 54–62.
[63] A.D. Bangham, R.W. Horne, Negative staining of phospholipids and their structural modification by surface-active agents as observed in the electron microscope, J. Mol. Biol. 8 (1964) 660–668.
[64] N. Düzgüneş, G. Gregoriadis, Introduction: The origins of liposomes: Alec Bangham at Babraham, Enzymology. Meth. Enzymol. 391 (2005) 1–3.
[65] A. Akbarzadeh, R. Rezaei-Sadabady, S. Davaran, et al., Liposome: Classification, preparation, and applications, Nanoscale Res. Lett. 8 (2013), 102.
[66] R. Tenchov, R. Bird, A.E. Curtze, et al., Lipid nanoparticles–from liposomes to mRNA vaccine delivery, a landscape of research diversity and advancement, ACS Nano 15 (2021) 16982–17015.
[67] A.C. Hortelão, S. García-Jimeno, M. Cano-Sarabia, et al., LipoBots: Using liposomal vesicles as protective shell of urease-based nanomotors, Adv. Funct. Mater. 30 (2020), 2002767.
[68] V.D. Nguyen, H.-K. Min, C.-S. Kim, et al., Folate receptor-targeted liposomal nano complex for effective synergistic photothermal-chemotherapy of breast cancer *in vivo*, Colloids Surf. B Biointerfaces 173 (2019) 539–548.
[69] S. Fu, Y. Zhao, J. Sun, et al., Integrin $\alpha_v\beta_3$-targeted liposomal drug delivery system for enhanced lung cancer therapy, Colloids Surf. B Biointerfaces 201 (2021), 111623.
[70] Z. Deng, Y. Xiao, M. Pan, et al., Hyperthermia-triggered drug delivery from iRGD-modified temperature-sensitive liposomes enhances the anti-tumor efficacy using high intensity focused ultrasound, J. Control. Release 243 (2016) 333–341.

[71] F. Pierigè, S. Serafini, L. Rossi, et al., Cell-based drug delivery, Adv. Drug Deliv. Rev. 60 (2008) 286–295.
[72] R.H. Fang, W. Gao, L. Zhang, Targeting drugs to tumours using cell membrane-coated nanoparticles, Nat. Rev. Clin. Oncol. 20 (2023) 33–48.
[73] Q. Xia, Y. Zhang, Z. Li, et al., Red blood cell membrane-camouflaged nanoparticles: A novel drug delivery system for antitumor application, Acta Pharm. Sin. B 9 (2019) 675–689.
[74] L. Gao, H. Wang, L. Nan, et al., Erythrocyte membrane-wrapped pH sensitive polymeric nanoparticles for non-small cell lung cancer therapy, Bioconjug. Chem. 28 (2017) 2591–2598.
[75] S. Tang, F. Zhang, H. Gong, et al., Enzyme-powered Janus platelet cell robots for active and targeted drug delivery, Sci. Robot. 5 (2020), eaba6137.
[76] E. Humphry, C.E. Armstrong, Physiology of red and white blood cells, Anaesth, Intensive Care Med. 23 (2022) 118–122.
[77] D. Wang, S. Wang, Z. Zhou, et al., White blood cell membrane-coated nanoparticles: Recent development and medical applications, Adv. Healthc. Mater. 11 (2022), e2101349.
[78] J. Zheng, R. Qi, C. Dai, et al., Enzyme catalysis biomotor engineering of neutrophils for nanodrug delivery and cell-based thrombolytic therapy, ACS Nano 16 (2022) 2330–2344.
[79] J. Cortes, C. Saura, Nanoparticle albumin-bound (nab^{TM})-paclitaxel: Improving efficacy and tolerability by targeted drug delivery in metastatic breast cancer, Eur. J. Cancer Suppl. 8 (2010) 1–10.
[80] A. Spada, J. Emami, J.A. Tuszynski, et al., The uniqueness of albumin as a carrier in nanodrug delivery, Mol. Pharm. 18 (2021) 1862–1894.
[81] S. Lamichhane, S. Lee, Albumin nanoscience: Homing nanotechnology enabling targeted drug delivery and therapy, Arch. Pharm. Res. 43 (2020) 118–133.
[82] H. Tian, J. Ou, Y. Wang, et al., Bladder microenvironment actuated proteomotors with ammonia amplification for enhanced cancer treatment, Acta Pharm. Sin. B 13 (2023) 3862–3875.
[83] Z. Liu, S. Liu, X. Zhao, et al., Photothermal-accelerated urease-powered human serum albumin nanomotor for rapid and efficient photothermal and photodynamic cancer combination therapy, Int. J. Biol. Macromol. 240 (2023), 124486.
[84] X. Ma, A.C. Hortelao, A. Miguel-López, et al., Bubble-free propulsion of ultrasmall tubular nanojets powered by biocatalytic reactions, J. Am. Chem. Soc. 138 (2016) 13782–13785.
[85] S. Sengupta, K.K. Dey, H.S. Muddana, et al., Enzyme molecules as nanomotors, J. Am. Chem. Soc. 135 (2013) 1406–1414.
[86] K.K. Dey, X. Zhao, B.M. Tansi, et al., Micromotors powered by enzyme catalysis, Nano Lett. 15 (2015) 8311–8315.
[87] A. Somasundar, S. Ghosh, F. Mohajerani, et al., Positive and negative chemotaxis of enzyme-coated liposome motors, Nat. Nanotechnol. 14 (2019) 1129–1134.
[88] N. Du, M. Chen, Z. Liu, et al., Kinetics and mechanism of jack bean urease inhibition by Hg^{2+}, Chem. Cent. J. 6 (2012), 154.
[89] B. Krajewska, W. Zaborska, M. Chudy, Multi-step analysis of Hg^{2+} ion inhibition of jack bean urease, J. Inorg. Biochem. 98 (2004) 1160–1168.
[90] M. Valles, S. Pujals, L. Albertazzi, et al., Enzyme purification improves the enzyme loading, self-propulsion, and endurance performance of micromotors, ACS Nano 16 (2022) 5615–5626.
[91] M. Luo, S. Li, J. Wan, et al., Enhanced propulsion of urease-powered micromotors by multilayered assembly of ureases on Janus magnetic microparticles, Langmuir 36 (2020) 7005–7013.
[92] Z. Yang, L. Wang, Z. Gao, et al., Ultrasmall enzyme-powered Janus nanomotor working in blood circulation system, ACS Nano 17 (2023) 6023–6035.
[93] S. Cao, H. Wu, I.A.B. Pijpers, et al., Cucurbit-like polymersomes with aggregation-induced emission properties show enzyme-mediated motility, ACS Nano 15 (2021) 18270–18278.
[94] W. Gao, S. Sattayasamitsathit, J. Orozco, et al., Highly efficient catalytic microengines: Template electrosynthesis of polyaniline/platinum microtubes, J. Am. Chem. Soc. 133 (2011) 11862–11864.
[95] R.A. Pavlick, S. Sengupta, T. McFadden, et al., A polymerization-powered motor, Angew. Chem. Int. Ed. Engl. 50 (2011) 9374–9377.
[96] W.F. Paxton, P.T. Baker, T.R. Kline, et al., Catalytically induced electrokinetics for motors and micropumps, J. Am. Chem. Soc. 128 (2006) 14881–14888.
[97] G. Zhao, M. Pumera, Macroscopic self-propelled objects, Chem. Asian J. 7 (2012) 1994–2002.
[98] T. Toyota, N. Maru, M.M. Hanczyc, et al., Self-propelled oil droplets consuming "fuel" surfactant, J. Am. Chem. Soc. 131 (2009) 5012–5013.
[99] L. Baraban, D. Makarov, R. Streubel, et al., Catalytic Janus motors on microfluidic chip: Deterministic motion for targeted cargo delivery, ACS Nano 6 (2012) 3383–3389.
[100] D. Folio, A. Ferreira, Modeling and estimation of self-phoretic magnetic Janus microrobot with uncontrollable inputs, IEEE Trans. Contr. Syst. Technol. 30 (2022) 2681–2688.
[101] J. Wu, D. Folio, J. Zhu, et al., Motion analysis and real-time trajectory prediction of magnetically steerable catalytic Janus micromotors, Adv. Intell. Syst. 4 (2022), 2200192.
[102] D. Vilela, U. Cossío, J. Parmar, et al., Medical imaging for the tracking of micromotors, ACS Nano 12 (2018) 1220–1227.
[103] T. Daeneke, K. Khoshmanesh, N. Mahmood, et al., Liquid metals: Fundamentals and applications in chemistry, Chem. Soc. Rev. 47 (2018) 4073–4111.
[104] K. Kalantar-Zadeh, J. Tang, T. Daeneke, et al., Emergence of liquid metals in nanotechnology, ACS Nano 13 (2019) 7388–7395.
[105] S. Kulkarni, A. Pandey, S. Mutalik, Liquid metal based theranostic nanoplatforms: Application in cancer therapy, imaging and biosensing, Nanomedicine 26 (2020), 102175.
[106] H. Song, T. Kim, S. Kang, et al., Ga-based liquid metal micro/nanoparticles: Recent advances and applications, Small 16 (2020), e1903391.
[107] S.A. Chechetka, Y. Yu, X. Zhen, et al., Light-driven liquid metal nanotransformers for biomedical theranostics, Nat. Commun. 8 (2017), 15432.
[108] Q. Wang, Y. Yu, K. Pan, et al., Liquid metal angiography for mega contrast X-ray visualization of vascular network in reconstructing *in-vitro* organ anatomy, IEEE Trans. Biomed. Eng. 61 (2014) 2161–2166.
[109] D. Xu, J. Hu, X. Pan, et al., Enzyme-powered liquid metal nanobots endowed with multiple biomedical functions, ACS Nano 15 (2021) 11543–11554.
[110] A. Refaat, M.L. Yap, G. Pietersz, et al., *In vivo* fluorescence imaging: Success in preclinical imaging paves the way for clinical applications, J. Nanobiotechnology 20 (2022), 450.
[111] H. Wang, Q. Li, P. Alam, et al., Aggregation-induced emission (AIE), life and health, ACS Nano 17 (2023) 14347–14405.
[112] G. Raposo, W. Stoorvogel, Extracellular vesicles: Exosomes, microvesicles, and friends, J. Cell Biol. 200 (2013) 373–383.
[113] E. Cocucci, J. Meldolesi, Ectosomes and exosomes: Shedding the confusion between extracellular vesicles, Trends Cell Biol 25 (2015) 364–372.
[114] R.J. Simpson, S.S. Jensen, J.W.E. Lim, Proteomic profiling of exosomes: Current perspectives, Proteomics 8 (2008) 4083–4099.
[115] R. Wubbolts, R.S. Leckie, P.T.M. Veenhuizen, et al., Proteomic and biochemical analyses of human B cell-derived exosomes. Potential implications for their function and multivesicular body formation, J. Biol. Chem. 278 (2003) 10963–10972.
[116] C. Subra, K. Laulagnier, B. Perret, et al., Exosome lipidomics unravels lipid sorting at the level of multivesicular bodies, Biochimie 89 (2007) 205–212.
[117] Q.-F. Han, W.-J. Li, K.-S. Hu, et al., Exosome biogenesis: Machinery, regulation, and therapeutic implications in cancer, Mol. Cancer 21 (2022), 207.
[118] X. Liu, Y. Wang, Y. Peng, et al., Urease-powered micromotors with spatially selective distribution of enzymes for capturing and sensing exosomes, ACS Nano 17 (2023) 24343–24354.
[119] W. Wang, C. Zhou, A journey of nanomotors for targeted cancer therapy: Principles, challenges, and a critical review of the state-of-the-art, Adv. Healthc. Mater. 10 (2021), e2001236.
[120] S. Antoni, J. Ferlay, I. Soerjomataram, et al., Bladder cancer incidence and mortality: A global overview and recent trends, Eur. Urol. 71 (2017) 96–108.
[121] P. Tyagi, P.-C. Wu, M. Chancellor, et al., Recent advances in intravesical drug/gene delivery, Mol. Pharm. 3 (2006) 369–379.
[122] Z. Zhang, D. Zhang, B. Qiu, et al., Icebreaker-inspired Janus nanomotors to combat barriers in the delivery of chemotherapeutic agents, Nanoscale 13 (2021) 6545–6557.
[123] J.C. Fraire, M. Guix, A.C. Hortelao, et al., Light-triggered mechanical disruption of extracellular barriers by swarms of enzyme-powered nanomotors for enhanced delivery, ACS Nano 17 (2023) 7180–7193.
[124] X. Li, J.F. Lovell, J. Yoon, et al., Clinical development and potential of photothermal and photodynamic therapies for cancer, Nat. Rev. Clin. Oncol. 17 (2020) 657–674.
[125] Y. Hou, X. Yang, R. Liu, et al., Pathological mechanism of photodynamic therapy and photothermal therapy based on nanoparticles, Int. J. Nanomedicine 15 (2020) 6827–6838.
[126] C. Donohoe, M.O. Senge, L.G. Arnaut, et al., Cell death in photodynamic therapy: From oxidative stress to anti-tumor immunity, Biochim. Biophys. Acta Rev. Cancer 1872 (2019), 188308.
[127] C.J.L. Murray, K.S. Ikuta, F. Sharara, et al., Global burden of bacterial antimicrobial resistance in 2019: A systematic analysis, Lancet 399 (2022) 629–655.
[128] D. Vilela, N. Blanco-Cabra, A. Eguskiza, et al., Drug-free enzyme-based bactericidal nanomotors against pathogenic bacteria, ACS Appl. Mater. Interfaces 13 (2021) 14964–14973.
[129] H. Wei, L. Yang, C. Pang, et al., Bacteria-targeted photothermal therapy for combating drug-resistant bacterial infections, Biomater. Sci. 11 (2023) 5634–5640.
[130] D.M. Wootton, D.N. Ku, Fluid mechanics of vascular systems, diseases, and thrombosis, Annu. Rev. Biomed. Eng. 1 (1999) 299–329.
[131] B. Furie, B.C. Furie, Mechanisms of thrombus formation, N. Engl. J. Med. 359 (2008) 938–949.
[132] S. Zhang, C. Zhu, W. Huang, et al., Recent progress of micro/nanomotors to overcome physiological barriers in the gastrointestinal tract, J. Control. Release 360 (2023) 514–527.
[133] J.P. Celli, B.S. Turner, N.H. Afdhal, et al., *Helicobacter pylori* moves through mucus by reducing mucin viscoelasticity, Proc. Natl. Acad. Sci. USA 106 (2009) 14321–14326.
[134] D. Walker, B.T. Käsdorf, H.-H. Jeong, et al., Enzymatically active biomimetic micropropellers for the penetration of mucin gels, Sci. Adv. 1 (2015), e1500501.
[135] S. Tenzer, D. Docter, J. Kuharev, et al., Rapid formation of plasma protein corona critically affects nanoparticle pathophysiology, Nat. Nanotechnol. 8 (2013) 772–781.
[136] S. Wilhelm, A.J. Tavares, Q. Dai, et al., Analysis of nanoparticle delivery to tumours, Nat. Rev. Mater. 1 (2016), 16014.